SEISMIC PERFORMANCE OF TWO FULL SIZE REINFORCED CONCRETE BEAM-COLUMN JOINT UNITS

R.W.G. Blakeley*, L.M. Megget**, M.J.N. Priestley***

SYNOPSIS

The design, construction and testing of two large reinforced concrete beam-column assemblies, representing an interior and an exterior joint, are described. Member details were based on an actual frame building designed by the M.W.D. Extensive results are presented which indicate very satisfactory behaviour particularly in the joint region. Hinges formed in the beams in all cases, and stable behaviour was obtained at displacement ductility factors of up to 6 and 8 for the interior and exterior test units respectively. Results are assessed in terms of design assumptions, and tentative design recommendations are made.

1. INTRODUCTION

1.1 Background to Tests

The approach to good detailing of beam-column joints for seismic resistance is a problem which currently assumes major importance for the designers of reinforced concrete frames. A considerable research effort has been directed towards solving this problem, notably by Hanson and Conner of the Portland Cement Association [1,2,3], Park, Paulay and others of University of Canterbury [4,5], and by Japanese investigators [6,7], to name but a few. This work has already been summarised recently by Bertero [8]. Many of these tests have shown that seismic type loading can induce yielding of the joint ties followed by loss of integrity of the joint and substantial degradation of strength and stiffness. This has been evident for both interior and exterior beam-column assemblies. In some cases where the joint has behaved satisfactorily [2] the performance has been helped by column axial loads as high as one-third of the column capacity, which will be unrepresentative for many parts of the frame, or by imposed rotations rather less than would be incurred under severe earthquake loading.

Testing has generally been on planar assemblies, sometimes with transverse beam stubs, and there is clearly a need for information on the performance of three dimensional assemblies subjected to simultaneous flexing in each principal direction. Also, most of the tests have been conducted on specimens which could not be regarded as full size according to current New Zealand design practice, particularly for Zone A, and verification is needed on possible influence of size effects, especially the relationship between bar diameter and member size.

Concern at the research results has led some designers to detail beam-column joints with heavy concentrations of ties and there have been associated construction difficulties. The objective of this series of tests was initially to establish if the deficiencies demonstrated previously still exist in a conventionally detailed specimen which could be regarded as full size according to contemporary practice. If performance was still unsatisfactory the series was intended to investigate innovative joint details as a solution. Ultimately, the series could be extended to consider the effect of concurrent beam hinging on the behaviour of the beam-column joints in a three-dimensional assembly. Close liaison has been maintained with University of Canterbury to ensure that current research is complementary. The results reported are from the initial part of the programme. On the basis of these results tentative recommendations are made for the design of joint reinforcement.

1.2 Theory of Joint Behaviour

1.2.1 Code Requirements

The approach recommended for the shear design of beam-column joint reinforcement in current codes such as ACI 318-71 [9] and SEAOC [10] is based on that for shear design of beams or columns, whereas both the applied shears and the mechanism of shear resistance is rather different in the case of beam-column joints. The design shear from Appendix A of ACI 318-71 is to be computed "by an analysis taking into account the column shear and the shears developed from the yield forces in the beam reinforcement". The shear reinforcement is to be proportioned according to the requirements for columns, which include an allowance for some shear to be carried by the concrete and assumes that diagonal tension cracks form at an angle of 45^{o} to the axis of the member.

* Design Engineer, Office of the Chief Structural Engineer, M.W.D. Head Office.
** Senior Engineer, Office of the Chief Structural Engineer, M.W.D. Head Office.
*** Senior Lecturer, University of Canterbury, previously Head, Structures Laboratory, M.W.D. Central Laboratories.

1.2.2 Shear Transfer Mechanisms

The actual internal forces imposed on the joint due to the external actions are illustrated in Fig. 1 for both interior and exterior beam-column joints. The concentrated tension and compression forces in both beam and column, minus the much smaller values of column and beam shears, induce the resultant diagonal tension and compression stresses in the panel zone of the joint. These stresses can be very high at yield conditions in the members and give rise to a number of diagonal tension cracks. Several investigators [3,4] have shown that these cracks pass from corner to corner across the joint and not at 45° as has sometimes been assumed. Under cyclic loading the diagonal tension cracks open and close in each direction as the direction of load alternates. If these cracks become too wide resulting from yield of the transverse ties the relative shear displacements along the crack can lead to uneven bearing followed by grinding of the concrete and general deterioration of the joint.

Shear transfer across the panel zone of joints may be attributed in varying proportions to the mechanisms of either arch or truss action. Of the two, arch action is the more efficient. Figs. 1 (a) and (c) illustrate the compressions induced by flexure in the concrete of the beam and column being transferred directly across the joint by a diagonal concrete arch. On the other hand, those forces which are induced in the panel zone through bond to the reinforcing bars must be transferred by a truss mechanism comprising a number of diagonal compression struts in the concrete and tension ties in the steel. Typical members in this mechanism are illustrated in Fig. 1 (b). In a conventional joint the horizontal ties are provided by transverse stirrups but the required vertical ties are apparently absent. The vertical component of some diagonal compression struts can be resisted in the compression zones of the column, but elsewhere the only members that may contribute to this function are the column bars. Since these will usually be only around the perimeter they are unlikely to be as effective as would be restraint of the beam flexural steel by corners of vertical stirrups. For full truss action to be developed a system of horizontal and vertical ties appears necessary. Transverse ties at right angles to the shear ties are also required to confine the concrete of the diagonal compression struts to retain their load carrying capacity.

Although concrete arch action is clearly desirable, the shear is transferred primarily by a truss mechanism in many joints. This is particularly true where the column axial load is low or where a steel couple forms in the beam under reversed cyclic loading. Joint details which promote arch action, such as the use of prestressing tendons at mid-depth of the beam or welding mechanical anchorages to the reinforcing bars at the beam or column interfaces appear attractive. Other details which remove the need for truss action, such as bending the longitudinal reinforcement in members diagonally across the joint, could be investigated.

1.2.3 Bond Forces on Flexural Steel

An aspect of the joint problem integrally associated with shear is the anchorage of the flexural reinforcing bars. For example, a force equal to the sum of the tensile and compressive yield forces in a beam reinforcing bar can be required to be transferred by bond over a length equal to the depth of the column. This is usually much less than the minimum anchorage length required by codes, and the problem is compounded by the fact that there may be good bond conditions only over a fraction of the column depth. As illustrated in Figs. 1 (a) and (c), the only zones of good bond resistance for beam bars are beneath the compression zones of the column. The horizontal ties enhance the bond transfer capacity for the vertical column bars, but no such advantage exists for the horizontal beam bars in a conventional joint. Under cycles of reversed loading bond may thus be lost from the beam bars in the region of the column flexural tension and beam steel yielding may progress some distance into the joint beyond the column face. Yielding may progress back from the other column face when loading is reversed, and finally there could be loss of bond throughout the joint associated with severe splitting and reduced flexural capacity of the beam as observed by Park and Thompson [5]. Behaviour may be helped in external beam-column joints if the bond forces extend back to the bend where the radial forces tend to promote desirable arch action.

2. DESIGN

2.1 Prototype Building

The test specimens were based on a Standard Minitech. Teaching Block structure designed in the Hamilton District Office of the Ministry of Works and Development. This prototype structure is a 3 by 3 bay, 4-storey frame with external spans of 8.839m, internal longitudinal span of 11.430m and internal transverse span of 8.382m and the inter-storey height is 3.658m throughout. The structural system is an in-situ, 2-way, ductile reinforced concrete frame with 356mm deep prestressed, precast double T-slabs with a 76mm concrete topping. The roof is a steel truss with light roofing materials. All columns are 686mm square; first to third floor beams are 889mm deep by 457mm wide; and the roof beams are 686mm deep by 457mm wide.

The prototype was designed using the new draft loading code; DZ 4203 [11] as a framed public building situated in seismic Zone A. Design and reinforced concrete detailing were to the contemporary practice of the MWD based on NZS 3101P [12] and MWD Code of Practice, "Design of Public Buildings" PW 81/10/1, [13].

2.2 Test Units

2.2.1 Member Properties

The details of the full-sized units were taken from those of the prototype at the first floor level and comprised an interior and exterior joint. Figs.

2 (a) and 2 (b) show the sizes and reinforcement details of the interior and exterior joints respectively. The 4.420m beam length to the loading pivot represents half the 8.839m external span.

2.2.2 Beam Design

The prototype had beam reinforcing in single layers due to the precast slab restrictions which required the main bars to be of size D32. It was considered that D32 beam bars should be avoided with a column of this size where possible because of their severe bond demands in the joint region. Thus, for the purposes of a representative test unit, the sections were redetailed using 28.6mm (No. 9) bars as the largest diameter and two layers of top steel in the interior joint. At the time of fabrication of the test units 13mm (4Ø) ties as used in the prototype beam were not available and the design was amended to pairs of 10mm (3Ø) rectangular ties at 152mm centres. The concrete was assumed to have no shear carrying capacity in the plastic hinge zones of two times the effective beam depth from the face of the column. The tie spacing satisfied the Code [9] minimum of d/4 and was less than six times the diameter of the main reinforcement which is desirable if buckling of the compression reinforcement is to be avoided under severe curvature reversals [14]. Where design allowed shear reliance on the concrete the stirrup-tie spacing was doubled. The stirrup-tie positioned near the column-face was within the concrete cover, as near to the column reinforcement as was possible. The ACI Code [9] specifies the first stirrup-tie within 76mm of the column face but this seems excessive as major cracking occurs in the column cover concrete at the beam-column interface.

It was decided not to place transverse beam stubs on the specimens as these may give unrealistic advantage to the joint performance. Under normal seismic conditions frames will deform biaxially and full-depth cracks may form at the beam-column interface in both directions, so reducing the confining effect of the transverse beams. Note that in both units the transverse beam bars were placed in the joint to simulate the practical difficulties of placing concrete through a mesh of beam steel.

The cover concrete to the bottom beam bars was the worse case of the prototype beams in both directions. Large covers were required to keep both beam depths equal. Note that the amount of bottom beam reinforcement was a little more than half of the top reinforcement in compliance with the code. The beam bar anchorage in the exterior joint specimen was accomplished with U-bars and L-bars projecting out of the far column face into a 152mm long beam stub.

2.2.3 Joint Design

The joint shear ties were redesigned for the test units. The procedure used probably represents an upper limit of contemporary joint design practice, but it was considered imperative that joint shear failure be averted if adequate information on the joint shear mechanism was to be derived from the tests. The maximum shear in the joint was calculated assuming yielding of the beams in the direction being considered (not biaxial), taking a 25% overstrength yield stress of 345 MPa in the beam reinforcing. From that force the column shear in the actual test units, with the beams yielding, was subtracted to obtain the horizontal joint shear. Reinforcement for this shear was calculated neglecting any shear carried by the concrete and using a tie steel yield stress of 276 MPa and capacity reduction factor for shear, $\emptyset = 0.85$. It was also assumed that only 2/3rds of the joint ties were effective in carrying shear. This follows results in previous tests where not all the joint ties crossing the critical corner to corner crack have yielded [4]. It should be noted that the concession in some codes (9,10), allowing reduction of the transverse steel in an interior joint by one half, was not used as the validity appears questionable. In the interior joint ten sets of 19mm dia. ties (6Ø) were required. Each set comprised three ties per set, with the 4 full-length tie legs assumed effective across any uniaxial diagonal crack, refer Fig. 2. To effectively hold all internal column bars by a 90° bend of a tie, the rectangular internal ties were displaced one column bar from the corresponding tie of the set above and below. The intention of this detail was to ensure confinement of the joint concrete, through arching action to the main bars. Six sets of 19mm (6Ø) ties (2 rectangular and one square tie per set) were required to carry the joint shear in the exterior joint. As the maximum spacing of confining hoops specified is 100mm [13], 7 sets of 19mm ties were detailed between the top and bottom beam reinforcement. All joint ties were designed with single-flare Vee groove lap welds mid-way along a long side with a minimum weld length of 130mm.

If biaxial yielding of all the beams had been considered in design, approximately double the amount of joint ties would have been required [15]. Placement of these ties would have proved impossible in the interior joint without going to a deeper beam section.

2.2.4 Column Design

The "weak beam-strong column" approach was used throughout the design of the prototype. The column reinforcement was determined from capacity design principles for concurrent yielding of beams in the two principal axes at a joint. Although the columns were designed for concurrent beam yielding but only tested under uniaxial yielding, the reinforcement was not reduced since these were not critical members for these tests.

The interior joint unit's column transverse reinforcement was identical to that in the prototype, namely pairs of square and octagonal 19 mm dia. (6Ø) ties at 102mm centres. This arrangement has the advantage of providing reasonable support for the longitudinal steel, while leaving a clear central passage for concrete placement. To eliminate any strain-ageing effects, the half octagonal ties were heat treated to British Standard Specifications

(16). The two half octagonal ties and the square tie were then single flare Vee groove welded together. Heat treatment was felt warranted due to the proximity of the weld to the 45° bend in the octagonal tie pieces. While recent tests (17) have shown no strain-ageing effects, it was considered that in this case heat treatment was expedient in order to eliminate any possibility of premature failure in a non-critical member.

One square and two rectangular ties were substituted in the exterior column to allow a uniform tie pattern throughout the column length. The different tie pattern used from that in the interior column was caused in part by the smaller number of main column bars. The constant axial load applied to the interior joint throughout the test was $0.05f_c'Ag$ (620 kN). This represents the minimum axial load on a prototype interior column at lower levels under dead and live load reduced by 30% for vertical earthquake accelerations, together with maximum upward beam shears derived from uneven interior span lengths. No axial load was applied to the exterior column specimen because under the above load condition the prototype exterior intermediate column would be carrying only $0.01f_c'Ag$ and the corner column would be carrying a tension axial load. Although column axial loads change substantially during an earthquake, the test column loads were kept constant at their approximate minimum as this creates critical conditions for bond within the beam-column joint.

3. TEST DETAILS

3.1 Construction Methods

Testing was carried out in the Structures Laboratory of the M.W.D. Central Laboratories. Construction methods and tolerances were to M.W.D. Concrete Major Works Specifications, Dec. 1970. Steel was supplied bent to shape by a steel fabricator, concrete was supplied by a ready-mix contractor and placed by concrete pump, and boxing built in the laboratory was of typical design and dimensional accuracy. Reinforcing cages were assembled by laboratory staff. It was found that positions of the column tie-sets in the interior joint differed by up to 25 mm from specified positions, due to congestion resulting from the use of vertically aligned rather than horizontally aligned welded laps on the internal ties.

Each test unit was cast upright in two pours with a construction joint in the column at the level of the beam top. In the first pour, concrete was initially placed in the column to the level of the beam soffit, the beam concrete was then placed, the column revibrated and concrete for the joint placed last. Despite difficulty in placing the joint concrete final appearance of the test units was good, with no sign of late settlement of concrete in the column. Boxing was struck at 24 hours, and surfaces were coated with a proprietary membrane curing compound. Full test details are given elsewhere (18).

3.2 Material Properties

3.2.1. Concrete

Six 200 x 100 mm diameter cylinders were moulded from the concrete placed at each area of specific interest (joint; beam concrete adjacent to joint) and given standard curing. Tests for compression strength were carried out at 28 days, and compression and tensile splitting strengths, together with the Modulus of Elasticity, were measured at the time of testing the joint units. Mix details and test results are summarised in Table 1. Compression strength was more than 50% higher than the specified 28 day minimum value of 27.5 MPa.

3.2.2. Steel

All reinforcing bars of a particular size were taken from the same steel batch. Five samples were cut from each size, straingauged with the same gauges intended for use on the joint bars, and tested in tension to establish stress-strain characteristics. Fig. 3 shows the average curves for beam and column main steel up to 6% strain. Note the comparatively short yield plateaux, with yield strain ratios of 13.6, 11.3 and 10.7 at the onset of strain hardening, for the 25.4 mm (No. 8), 28.6 mm (No. 9), and 31.8 mm (No. 10) bars respectively. Yield and ultimate stresses for all bar sizes are included in Table 1.

3.3 Load Application and Reaction

The base and top of the column for each test unit were connected through pivots to a reaction pad and reaction frame respectively, bolted to a reinforced concrete strong floor. Load was applied to the beam ends by independent hydraulic systems providing downward load (negative or hogging moment) through a straingauged tension yoke, and upward load through a compression load cell and rocker/roller system. For the interior joint, the reaction frame supporting the column-top pivot also contained a strong-back for reacting the required axial load of 0.05 fc' Ag (620 kN) where Ag = gross area of the column, supplied by a third hydraulic system consisting of two jacks in parallel. No axial load was applied to the exterior joint column. Fig. 4 shows in schematic form the test set-up for the interior joint. A photograph of the interior joint under test is given in Fig. 5.

3.4 Instrumentation

3.4.1 Deflections and Rotations

Beam end deflections were measured optically, sighting through surveying levels onto deflection scales attached to each tension yoke, to a precision of 0.1 mm. Beam rotations over successive d/2 gauge lengths adjacent to the column face, where d = effective depth were measured by 50 x .01 mm dialgauges. Horizontal column displacements were recorded at 6 locations by 20 x .01 mm dialgauges.

Demountable mechanical straingauges of 250 mm gauge length were used to record diagonal strains on both sides of the joint panel. From these, joint shear rotations could be calculated. Fig. 4 includes a general description of deflection and rotation gauges.

3.4.2 Steel Strains

Extensive use was made of electric resistance straingauges to monitor strains of beam and column flexural reinforcing, and of column ties within the joint region. On the beam steel, where steel strains in excess of 3% were anticipated, 6 mm Kyowa KLM-6-A9 high yield straingauges were used. Column bars and joint ties were gauged with 3 mm TML FLA-3-11 gauges.

On the basis of preliminary trials a system of moisture and mechanical protection consisting of a flexible layer of Bostik 1181 Contact Adhesive surrounding the gauge and terminal strip overlain by a hard shell of Expandite '5 Minute Epoxy' was adopted. Care was taken to keep the area of water-proofing small to minimise the possibility of significant bond loss. For the same reason, gauges were fixed to the underneath of the beam reinforcing bars where bond could be expected to be comparatively poor due to settlement, and gauge leads contained within electrical 'spaghetti' were physically separated from the reinforcing by spacers. Fig. 6 defines the straingauge locations for the two test units. In all, the interior and exterior units contained 175 and 160 straingauges respectively. In each case, all except two gauges survived the concrete placing and curing operations. Straingauges were connected to a 300 channel Dynamco Datalogger reading to 1 microstrain sensitivity with a range of ± 4% strain. Data was recorded on punched tape and analysed on the M.W.D.'s IBM 370/168 computer.

3.5 Test Sequence

Slightly different testing sequences were adopted for the two test units due to agreement within the M.W.D. subsequent to testing the first (interior joint) unit, on a standard test sequence for beam-column joints. The exterior joint test unit was tested in accordance with this sequence which is listed as an Appendix to this paper. The interior joint programme differed from this by the inclusion of a cycle at yield deflection, an additional cycle at a ductility factor of 4, and exclusion of 'elastic' cycles between sub-tests at specific ductility factors.

4. RESULTS

4.1 Interior Joint

4.1.1. Moment Deflection

The general behaviour of the interior joint is summarised in Fig. 7, which shows moment-deflection hysteresis loops for the two beams of the interior joint, together with a series of photographs showing physical condition of the beams and the joint panel at successively increasing ductility factors. Fig. 7 also indicates three moment limits, designated MY, MU.003 and MU.004 which represent the theoretical moment at which steel strains first reach yield, and the ultimate moments based on extreme fibre compression strains of 0.3% and 0.4% respectively. The difference between the two ultimate moments results largely from the degree of strain hardening of the tension steel, which was based on the measured stress-strain curves of Fig. 3.

Very satisfactory behaviour is exhibited in Fig. 7, with only minor load and stiffness degradation occurring at displacement ductility factors (DF) of 2, 4 and 6. Maximum negative moments for both beams fell within the range defined by the theoretical ultimate capacities MU.003 and MU.004, but maximum positive moments consistently exceeded MU.004 at ductility factors of 4 and higher. Degradation at DF = 8 was comparatively rapid and resulted from loss of cover from the beam concrete and buckling of the compression steel (see Fig. 8) preceded at an early stage of testing by bond cracking along the beam steel. Within the beam hinge regions, vertical crack patterns through the complete depth of the beams suffered shear displacement of ± 20 mm in the latter stages of testing. The joint panel remained in excellent condition throughout testing, as indicated by Fig. 9 which shows the condition after completion of testing.

The components of the West beam end displacement resulting from beam rotation and joint shear rotation for DF=2 to DF=8 are shown in Fig. 10. It will be seen that the largest contribution came from rotation in the first d/2 gauge length, where rotational ductility factors of 19 were measured at DF=6. Note the increase in stiffness as moments approach peak values, resulting from closing of cracks. The joint shear contribution is negligible at the higher ductility factors. Rather erratic curves from the second rotation gauge length at high ductility factors resulted from the high shear movements along cracks, and general structural degradation.

4.1.2. Steel Stresses

(a) Joint Ties

Fig. 11 shows the vertical distribution of longitudinal stresses measured in the joint tie sets at yield, and at DF=6. Although the scatter is considerable, average tie stresses were in the vicinity of 50 MPa at yield displacement, and 120 MPa at DF=6. The distribution at DF=6 includes a stress envelope with a peak stress of 195 MPa, or 66% yield containing all except two gauge readings which indicate yield at locations close to the bottom of the West top: East bottom diagonal. No consistent variations of stress between gauges on the two diagonals, shown separately by crosses and circles, was apparent, reflecting the uniform crack pattern throughout the joint panel. The stress distributions in Fig. 8 refer only to moment peaks with M_W negative and M_E positive, but behaviour was essentially the same for the reversed moment condition.

Confinement stresses indicated by strain gauges on transverse tie-legs were in most cases less than 100 MPa, but at large deformations the short tie-legs adjacent to the beam ends approached yield. As would be expected, these short ties were more effective than the square ties in resisting the bursting forces arising from diagonal compression in the panel zone.

(b) Column Bars

Stress distributions along column

bars through the joint region are shown at first yield and at DF=6 in Fig. 12. It will be noted that considerable non-linearity exists, particularly for bar 4, presumably as a result of carrying vertical tension stresses across joint cracks. It should be pointed out that similar behaviour could have been experienced by bar 2, with the reduced number of straingauges on this bar resulting in the stress peaks apparent on bar 4 being missed.

(c) Beam Steel

Apart from locations close to the column centreline, most beam strain gauges exceeded yield strain at an early stage of the test programme. Strains were converted to stresses using a Bauschinger analysis computer programme developed by Megget [19] from theoretical equations based on Ramberg-Osgood functions developed by Kent [20]. A typical stress-strain history for one strain gauge is given in Fig. 13. Note the tendency for the hysteresis loops to centre on successively higher average tensile strains at higher ductility factors. This is a natural result of the imbalance between positive and negative reinforcing percentages in the beams. Under negative moment high steel tension strains were developed in the top steel. On moment reversal the bottom steel had sufficient tensile capacity to yield the top steel in compression only if extensive strain hardening occurred, thus limiting the compression strains. A side effect of this was for each beam to 'grow' about 40 mm longer during testing.

Fig. 14 shows beam steel stress distributions through the joint at yield, DF = 2, 4 and 6, based on the Bauschinger analyses. It will be seen that stress distributions within the joint are close to linear, that yield progressed a maximum distance of approximately 150 mm within the joint, and that bond conditions were adequate to allow exceedingly high stress gradients to develop. As testing progressed, gauges on the beam steel outside the joint panel successively failed. In the case of the West Beam bottom steel, this resulted in a total loss of readings outside the joint panel subsequent to DF = 2.

Comparison of moments calculated from the steel stresses with applied moments gives a good indication of the accuracy of the Bauschinger analyses. For the eight cases given in Fig. 14, the average ratio of $M_{exp.}/M_{applied}$ was 0.995, with a range of 0.904 to 1.05.

4.2 Exterior Joint

4.2.1. Moment-Deflection

The moment-deflection behaviour of the exterior joint beam is given in Fig. 15, which includes photographs showing condition at increasing ductility factors. The designated moment limits have the same meaning as for Fig. 7. It will be seen that general behaviour is similar, even somewhat better, than that exhibited by the interior joint.

The test unit showed very satisfactory performances up to DF = 6. At DF = 8 almost total loss of bottom steel cover concrete occurred after the completion of two cycles (see photograph), but stiffness and moment capacities had not been significantly influenced by this stage. Peak negative moments at DF = 6 and DF = 8 agree well with the theoretical MU.003 value, while maximum positive moments exceed the MU.004 value by up to 10%. At DF = 10 severe buckling of the bottom steel bars occurred under negative moment in a manner similar to that displayed by the interior test unit in Fig. 8. By this stage the beam was sustaining large shear movements along major flexural cracks, and severe structural degradation was occurring. Note the significant stiffness degradation of the successive 'elastic' 3/4 yield cycles. Testing was terminated at the end of the DF = 10 sub-test. Fig 16 shows the condition of the test unit after completion of testing. The excellent condition of the joint panel should be noted.

Components of beam end-deflection resulting from beam rotation and joint shear rotation are presented in Fig. 17. Although the two beam rotation components are of similar magnitude under negative moment, the first d/2 hinge length contributes about seven times more than the second d/2 hinge length, to the end-deflection under positive moment. The component of end-deflection resulting from joint shear rotation is insignificant at all stages of testing.

4.2.2. Steel Stresses

(a) Joint Ties

Joint tie stress distributions under peak negative moment are shown for DF = 2 and DF = 8 in Fig. 18. Because of the imbalance between beam top and bottom reinforcing percentages, negative moment induces the critical joint shears. Nevertheless, stresses are low throughout the joint, with the average curves showing maxima of 44 MPa and 76 MPa at DF = 2 and DF = 8 respectively. The envelope to the distribution at DF = 8 has a maximum value of 120 MPa, or 41% yield.

No significant confining action was noted from stresses measured on transverse tie legs.

(b) Column Bars

Fig. 19 shows column bar stress distributions through the exterior joint at DF = 2 and DF = 8. Bars 2 and 3 each show large tensile peaks within the joint region, indicating shear transfer by truss action.

(c) Beam Steel

Beam steel stress distributions through the joint at DF = 2, 4, 6 and 8 are shown in Fig. 20. As with the internal joint, stresses are based on Bauschinger analyses.

As with the interior joint, stress distributions are close to linear at all stages of loading, dropping to zero in the beam stub, implying virtually constant bond stress along the bars at each ductility level. Maximum recorded steel stresses indicate significant strain-hardening, particularly for the bottom steel bars, where peak stresses up to 340 MPa (1.23 fy) were obtained. The high stresses confirm the high positive moments applied. Gauge failure outside the joint region was again substantial at ductility factors higher than 4, particularly for the bottom steel bars.

5. ASSESSMENT OF RESULTS

5.1 Panel Zone Performance

5.1.1. Shear Resistance

The performance of the panel zones of the two units may be assessed on the basis of the shear transfer mechanisms postulated in section 1.2.2. Four mechanisms present are: direct concrete compressive arch action; a major truss system comprising the legs of the ties extending full depth of the joint and the beam and end column bars; a minor truss system comprising the short legs of the internal transverse ties and the beam and intermediate column bars; and aggregate interlock across the diagonal tension cracks.

The contribution of the major truss to resisting the beam induced joint shear at varying stages of loading in each unit is indicated in Table 2. The shear forces tabulated are the total horizontal joint shear, V_j, the shear force induced in the joint from bond to the top beam steel, V_{st}, and the shear force induced in the joint from bond to the bottom beam steel, V_{sb}. In each case the shear force due to flexure in the column has been subtracted from the concentrated forces due to the beam concrete and steel. The sum of the average tensile forces in the tie legs of the major truss system, ΣT, are listed for comparison. Note that in the interior joint under post-elastic deformations the major truss ties may be resisting as much as 80% of the experimental total horizontal shear. After the beam strength has degraded at DF = 8 this proportion is apparently even higher. In the exterior joint the contribution of the major truss is rather less, being approximately 50% of the total horizontal shear in large amplitude cycles. The shear forces due to bond to the beam bars have been tabulated as these show a more direct relationship to the forces induced in the joint ties than does the total horizontal shear, which may include a component due to compressive forces in the concrete of the beam.

The forces comprising the major and minor truss system at loading stages of DF = 6 for the interior joint and DF = 8 for the exterior joint are presented in Fig. 21. The values are, of course, subject to the limits of experimental accuracy. Forces transferred by the minor truss system were derived from strain readings on the short tie legs and intermediate column bars. From limited evidence, stresses in the short tie legs of the exterior joint appeared similar to those of the long tie legs. For the major truss the horizontal shears have been derived from the summation of the beam bar forces either side of the joint minus both the column shear and the contribution of the minor truss. The concrete compression force at the bottom of the beam has been assumed to be transferred across the joint by arch action. The vertical shears comprise the bond forces transferred from the column bars at either extremity of the column to the panel zone. These were computed from the slope of the column bar stress profiles of Figs. 12 and 19. The beam shear has not been deducted in this case since with wide cracks these shears are likely to be transferred only in the region of the beam bars. The direction of the diagonal compression struts may be assumed to be parallel to the corner-to-corner cracks. Inspection of Fig. 21 (a) shows good resolution of all forces in the interior joint within the major truss system, except for balancing of the vertical components of the diagonal compression struts. Bond forces to the intermediate column bars resist some of this vertical component, but it is not clear how the major portion is resisted. From Fig. 21 (b) it appears that a smaller proportion of the bond forces from the top beam steel of the exterior joint are transferred by truss action than for the interior joint. That portion of the force in the tension bars developed in the beam stub or in the compression zone of the column could well be transferred directly across the joint by arch action. The interior joint will have a lesser tendency to this action because yield penetration results in bond transfer being ineffective at either extremity. In each unit the balance of the shear force will be transferred through the concrete by aggregate interlock.

Several inferences can be made from these results with respect to the design of joint ties. The margins of safety against yield of any ties were 34% for the interior joint and 59% for the exterior joint. The yield strength of the No. 9 (28.6mm) beam bars used was 276 MPa, that is exactly the specified minimum yield. If the bars had a 25% overstrength the above margins would be reduced to 17% and 49% respectively. A margin of 15% appears appropriate for design, and therefore if prevention of yield of any ties is to be the design criterion the design approach used in this test series could not be relaxed in the case of the interior joint. The requirements could only be reduced if yield of some tie legs was considered acceptable in view of the scatter of stresses apparent in Fig. 11 (b). Also, some relaxation may be appropriate for a beam with equal top and bottom reinforcement where some of the compression force at both top and bottom of the beam acts through the concrete. In the case of the exterior joint a reduction in the number of ties used appears acceptable from a shear requirement, but here the critical design criterion was confinement as required by the ACI code [9]. The validity of these requirements should be assessed in a separate investigation.

5.1.2. Bond

The stresses in the beam bars passing through the joint generally showed a linear rate of change. This is despite the expectation of bond conditions being most favourable beneath the compression zone of the column. The bond stresses were very high, particularly when yield progressed into the joint after several post-elastic cycles. In the interior joint unit tensile yield advanced a maximum distance of 150mm inside the column face at DF = 8. The development length for twice yield force was then 500 mm and the maximum bond stress 8.0 MPa. In the exterior joint unit tensile yield advanced a maximum distance of 230 mm inside the column face at DF = 10. Steel stresses decreased towards zero just beyond the far face of the column, requiring a development length of 420 mm and a maximum bond stress of 4.3 MPa. There was no substantial degradation of beam bar anchorage across the joint during load reversals and the anchorage length beyond the 90^{o} bend carried negligible stress. Thus the extra anchorage provided within the beam stub was apparently not required for a column of the size of the test specimen.

From the earliest stages of loading the strain gauge readings on the joint ties immediately below the top beam bars and above the bottom beam bars indicated that these ties were sustaining tensions induced by bond from the adjacent beam bars. This is particularly evident in Fig. 11 (b) where a tie leg immediately above the bottom bars is at yield. Although at that load increment this gauge is in a compression zone, tension yield was first indicated in this tie at DF = 4 in the opposite direction of loading.

The bond forces to the column bars in each unit are indicated in Figs. 12 and 19. Clearly these bars are contributing to the joint shear resisting mechanisms and it is desirable that designers should space bars evenly around the perimeter of the column.

5.2 Beam Performance

A feature of the beam performance was the influence of the imbalance between top and bottom reinforcement. This lead to irreversible yielding of the top beam bars and successive widening of the cracks with increasing cyclic deformations. Large shear displacements across these cracks resulted. This was particularly so on the west arm of the internal joint where under initial upward loading a vertical flexural crack formed which remained throughout testing, leaving dowel action of the main bars as the only mode of shear transfer for large portions of the loading sequence. Another important influence on the performance of the beam was the loss of the cover concrete at the bottom of the beam after dissection by bond and flexural cracking. This allowed the beam bars to buckle inwards, being a path of lesser resistance then buckling vertically against the restraint of ties. Reduction of the tie spacing from 150mm to 100mm would have improved this behaviour by helping to retain the cover concrete. The test units were designed for the critical case of maximum cover to the bottom steel as explained in section 2.2.2.

Translation of the test results to behaviour in an actual structure requires consideration of the influence of a floor slab on the performance, particularly with respect to the widening cracks in the beam. On the one hand the slab-steel will tend to accentuate the imbalance between negative and positive steel. However, on the other hand the slab would be expected to exert some restraint against widening of the beam cracks unless substantial cracking and deterioration of the slab occurred. While the answer to this is not as yet clear, it would seem to be an advantage where possible for the negative and positive beam steel to be equalised.

6. CONCLUSIONS AND DESIGN RECOMMENDATIONS

6.1 The performance of the two beam-column assemblies satisfied the anticipated ductility demands of severe seismic loading. The units formed stable hysteresis loops at displacement ductility factors of 6 and 8 for the interior and exterior joint units respectively, while sustaining loads in excess of the theoretical ultimate. Degradation at higher amplitude loadings was confined to the beam plastic hinge regions. Throughout the test sequence joint cracks were controlled by elastic behaviour.

6.2 Assessment of the joint shear performance from average tie stresses gave good agreement with theory based on shear resisting truss mechanisms comprising all tie legs. The design of the interior joint was successful in avoiding yield of the ties despite the considerable experimental scatter of stresses within any tie set and the moderate variation of effectiveness of different tie sets. This scatter indicates the need for a considerably lower capacity reduction factor than is normally used. This was achieved in this design by using in addition to the normal capacity reduction factor of 0.85 a further factor of 2/3, resulting in a reasonable experimental margin of safety against yield of the ties. It is felt that it may be sufficient to design for the average tie stress at any level instead of the envelope, in which case a factor higher than the 2/3 used would be acceptable. Until this is confirmed by test results the authors cannot recommend this approach. Also, it is recommended that for simplicity in design the contribution of those tie legs that do not extend the full depth of the joint be neglected. Experiment showed that these ties form a sub-truss resisting approximately 10% of the joint shear. Performance of the exterior joint indicates that a rather less conservative shear design approach than that used would be acceptable. However, the critical design criterion for the ties in this joint was confinement according to code requirements. The validity of these requirements should be subject to further investigation.

6.3 The desirability of evenly spaced column bars around the perimeter of the column is clearly indicated by strain gauge results showing the contribution of these bars to truss action within the joint.

6.4 Although yield progressed along the beam bars as much as 150 mm beyond the column face in the interior joint, satisfactory transfer from compression to tension yield was available due to very high bond stresses. As this does not appear to conform to current theories of bond stress, further research is indicated. It would appear that in the exterior joint the larger column size helped eliminate the bond failures observed in previous tests on such units.

6.5 The confinement of the beam concrete by stirrups in the plastic hinge zone was inadequate, and a lower spacing than the value of 150 mm used in these tests is required.

6.6 A significant influence on the performance of the joint units was the imbalance between top and bottom beam reinforcement. This led to wide cracks forming in the beams with relative shear movements across the cracks and subsequent deterioration of the member, It would be advantageous, therefore, if top and bottom beam steel areas could be equalised.

7. ACKNOWLEDGEMENTS

The permission of the Commissioner of Works, N. C. McLeod, to publish this paper is acknowledged. Grateful acknowledgement is made of the advice and guidance received from O. A. Glogau, Chief Structural Engineer, M.W.D. and I.C. Armstrong, then Design Engineer, M.W.D. Special acknowledgement is made to K. J. Thompson, Post Graduate Student, University of Canterbury, for supplying Bauschinger coefficients.

8. REFERENCES

1. Hanson, N. W. and Conner, H. W., "Seismic Resistance of Reinforced Concrete Beam-Column Joints", Proceedings of American Society of Civil Engineers, Vol. 93, ST5, October 1967, pp. 533-560.
2. Hanson, N. W., "Seismic Resistance of Concrete Frames with Grade 60 Reinforcement", Proceedings of the American Society of Civil Engineers, Vol. 97, ST6, June 1971, pp. 1685-1700.
3. Hanson, N. W. and Conner, H. W., "Tests of Reinforced Concrete Beam-Column Joints under Simulated Seismic Loading", Portland Cement Association Research and Development Bulletin, 1972, pp. 1-11.
4. Park, R. and Paulay, T., "Behaviour of Reinforced Concrete External Beam-Column Joints under Cyclic Loading", Fifth World Conference on Earthquake Engineering, Paper 88, Vol. 1, Session 2D, Rome, June, 1973, pp. 772-781.
5. Park, R. and Thompson, K. J., "Behaviour of Prestressed, Partially Prestressed and Reinforced Concrete Interior Beam-Column Assemblies under Cyclic Loading: Test Results of Units 1 to 7", Research Report, Department of Civil Engineering, University of Canterbury, September 1974, 42 pp.
6. Muto, K., Hisada, T., Tsugawa, T., and Bessho, S., "Earthquake Resistant Design of 20 Storey Reinforced Concrete Building", Fifth World Conference on Earthquake Engineering, Paper 242, Vol. 2, session 5D, Rome, June, 1973, pp. 1960 - 1969.
7. Higashi, V. and Ohwada, Y., "Failing Behaviour of Reinforced Concrete Beam-Column Connection Subjected to Lateral Load", Memoirs of the Faculty of Technology, 19, Tokyo Metropolitan University, 1969, pp. 91 - 101.
8. Bertero, V. V., "Experimental Studies Concerning Reinforced, Prestressed and Partially Prestressed Concrete Structures and Their Elements", Introductory Report for Theme IV, Symposium on Resistance and Ultimate Deformability of Structures Acted on by Well Defined Repeated Loads, International Association for Bridge and Structural Engineering, Lisbon, 1973, pp. 67 - 99.
9. ACI Committee 318, "Building Code Requirements for Reinforced Concrete (ACI 318-71)", American Concrete Institute, Detroit, 1971, 78 pp.
10. SEAOC Seismology Committee, "Recommended Lateral Force Requirements and Commentary", Structural Engineers Association of California, 1973, 146 pp.
11. Standards Association of N.Z., DZ 4203/304, Draft NZ Standard for General Structural Design and Design Loadings, Part 4, "Earthquake Provisions".
12. Standards Association of N.Z., NZS3101P, "Code of Practice for Reinforced Concrete Design", Wellington, 1970, 149 pp.
13. Ministry of Works and Development, New Zealand, PW 81/10/1, Office of the Chief Structural Engineer, "Code of Practice for the Design of Public Buildings", May 1970, 39 pp. plus appendix.
14. Bresler, Boris, Letter to Prof. John Breen, University of Texas "Ductility of Columns in Reinforced Concrete Moment Resistive Frames", February 29, 1972, 4 pp.
15. Armstrong, I. C., "Capacity Design of Reinforced Concrete Frames for Ductile Earthquake Performance", Bull. N.Z. Soc. for Earthquake Engineering, Vol. 5, No. 4, December, 1972, pp. 133 - 142.
16. British Standards Institution: BS 1500: Part 1, 1958 "Fusion Welded Pressure Vessels for General Purposes, Carbon and Low Alloy Steels". 134 pp.
17. Stevenson, R. B., "Strain Ageing", Letter to Chief Structural Engineer, MWD, re tests performed at Central Laboratories, 29 May, 1974, File 81/30/5/3.
18. Priestley, M.J.N., "Testing of 2 Reinforced Concrete Beam Column Assemblies under Simulated Seismic Loading", Central Laboratories Report 5-75/1, January 1975.
19. Megget, L. M., "Exterior Reinforced Concrete Joints with and without Intersecting Beams under Seismic Loading", Bull. of I.I.S.E.E., Vol. II, 1973, pp. 115 - 167.
20. Kent, D. C., "Inelastic Behaviour of Reinforced Concrete Members with Cyclic Loading", Ph.D. thesis, University of Canterbury, 1969, 246 pp.

APPENDIX

PROPOSED STANDARD TEST SEQUENCE FOR BEAM-COLUMN JOINTS

Comparison of results from different beam-column tests has frequently been difficult because of variations in the definitions of ductility factor and in the actual test sequences adopted by different researchers. In an endeavour to rectify this, the definitions and test sequences adopted by the M.W.D. are presented below, together with comments explaining the reasons for the choices adopted. It is hoped that this might form a basis for discussion aimed at developing a standard test sequence acceptable to a wider group of researchers working in the field.

YIELD DISPLACEMENT

The yield displacement is the displacement of the test beam at a distance L/2 from the column centre, where L is the distance between column centres in the structure modelled, when the steel yield strain is first attained at any point.

EXPERIMENTAL DETERMINATION OF YIELD DISPLACEMENT

For reinforced concrete members it is recommended that the yield displacement be calculated by extrapolation of the measured load-deflection curve from a last experimental reading at approximately 3/4 of the theoretical yield load, where the yield load is based on measured steel and concrete properties. Yield displacement based on steel strains measured during testing can contain significant errors due to straingauge positions not coinciding with crack positions, with consequent reduction in steel stress by bond, and also due to normal experimental scatter of straingauge readings. Further, the yield displacement on subsequent reversed loading could be affected by the first load to yield, particularly where top and bottom steel percentages are different.

DISPLACEMENT DUCTILITY FACTORS

(a) Interior Beam-Column Joints

Where top and bottom steel percentages are equal, yield displacements in both loading directions are also equal, and no problem exists in defining the ductility factor. However, where different steel percentages result in different positive and negative yield displacements the situation is more complex. Consider a beam spanning between two internal columns. At high structure ductility, the beam will contain plastic hinges at each end, whose rotations must effectively be equal. Thus in a test joint, equal end displacements should be imposed in both loading directions. This implies that for a specified member ductility factor, the imposed displacements should be based on the average of the positive and negative yield displacements. Note that different ductility requirements will result for the two loading directions.

(b) Exterior Joint

By similar reasoning, the ductility requirements of the end of a beam adjoining an exterior column will be influenced by the interior joint at the other end of the beam. Again, virtually equal rotations are required at each end, and the most appropriate choice of yield displacement for assessing ductility factors will be

$$y_e = \frac{(D_{ep} + D_{en} + D_{ip} + D_{in})}{4}$$

where D = magnitude of yield displacement
e = exterior joint
i = interior joint
p = positive
n = negative

This choice of definition will only be possible when the test programme included both interior and exterior joints. If this is not the case, theoretical values for D_{ep}, D_{en}, D_{ip} and D_{in} should be calculated and used to modify the experimental yield displacement based on an exterior joint only, as follows

$$y_e = \frac{(D_{ep} + D_{en})\ \text{exp.}}{4} \times \frac{(D_{ep} + D_{en} + D_{ip} + D_{in})\ \text{theor.}}{(D_{ep} + D_{en})\ \text{theor.}}$$

STANDARD TEST SEQUENCES

As shown in Fig. A-1, the agreed standard sequence consists of two initial 'elastic' cycles at 3/4 of yield load in each direction. Yield displacements are based on extrapolation of the load-deflection curves to the theoretical first-yield load. Subsequent testing comprises a series of sub-tests each consisting of two full cycles at a specified ductility factor followed by one complete cycle at 3/4 yield displacement, with the specified ductility factor starting at 2, and increasing by 2 in each successive sub-test. Thus behaviour of the test joint is investigated during a series of earthquakes of increasing intensity. The intermediate cycles at 3/4 yield displacement provide information on the 'elastic' response subsequent to an earthquake, while representing more closely the real situation of earthquake response, where not all cycles are post-elastic.

If severe structural degradation occurs at an early stage of testing, the number of cycles at the current ductility factors should be increased, rather than terminating after two cycles and moving to the next sub-test.

TABLE 1.

MIX PROPORTIONS AND MATERIAL PROPERTIES

MIX PROPORTIONS Kg/m^3		CONCRETE PROPERTIES			REINFORCING STEEL PROPERTIES		
			INTERIOR JOINT	EXTERIOR JOINT	BAR SIZE (mm)	YIELD STRESS MPa	ULTIMATE STRESS MPa
Gravel 13mm - 19mm	445	fc' 28 days	42.8 MPa	44.0 MPa	12.7 deformed	305	508
Gravel 13mm	445	fc' at testing	48.5 MPa	48.0 MPa	15.9 deformed	295	443
Sand	854	ft (splitting) at testing	4.3 MPa	4.1 MPa	25.4 deformed	299	469
Cement	332	E at testing	29.7 GPa	30.5 GPa	28.6 deformed	276	457
Water	190	Density	$2.39 kg/m^3$	$2.39 kg/m^3$	31.8 deformed	289	464
		Slump	160 mm	125 mm	9.53 round	322	494
					19.1 round	297	483

TABLE 2.

JOINT SHEARS AND TIE FORCES

INTERIOR JOINT						EXTERIOR JOINT					
Increment	V_j kN	V_{st} kN	V_{sb} kN	ΣT kN	$\frac{\Sigma T}{V_j}$	Increment	V_j kN	V_{st} kN	V_{sb} kN	ΣT kN	$\frac{\Sigma T}{V_j}$
+¾	770	486	221	273	0.35	+¾	665	665	77	22	0.03
-¾	644	378	111	245	0.38	-¾	555	46	555	0	0.00
+1	1140	526	361	629	0.55	+2	976	976	129	84	0.09
-1	1311	743	355	631	0.48	-2	773	773	773	148	0.19
+2	1347	1012	302	943	0.70	+4	1062	1062	368	308	0.29
-2	1430	1430	948	888	0.62	-4	804	804	804	205	0.25
+4	1440	1440	1020	1154	0.80	+6	1066	1066	378	320	0.30
-4	1677	1677	870	1161	0.69	-6	831	831	831	410	0.49
+6	1722	1722	1124	1293	0.75	+8	1104	1104	391	364	0.33
-6	1685	1685	991	1335	0.79	-8	770	770	770	456	0.59
+8	1494	1494	941	1238	0.83	+10	1008	1008	360	340	0.34
-8	1347	1347	851	1398	1.04	-10	844	844	400	400	0.48

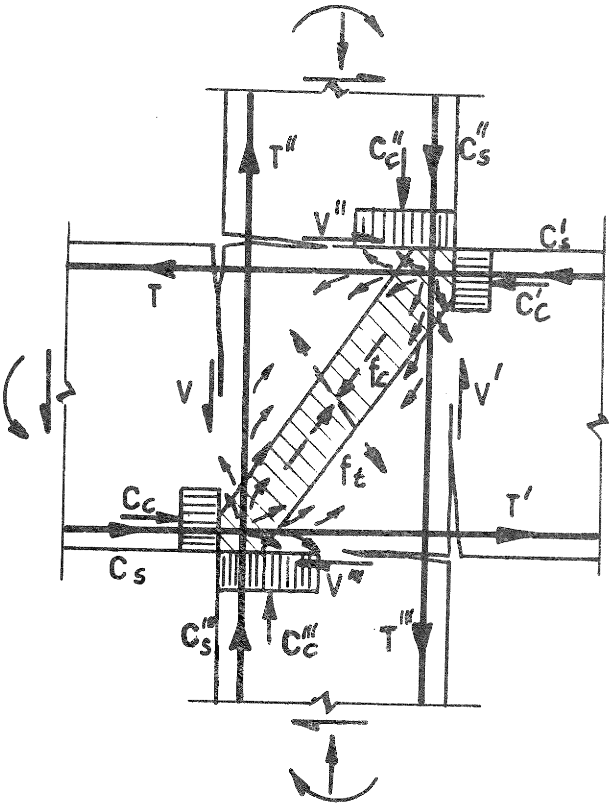

(a) Forces on Internal Joint

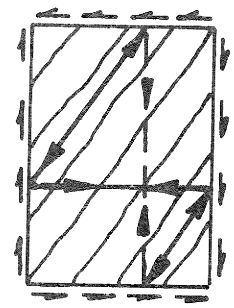

(b) Panel Zone Truss Mechanism

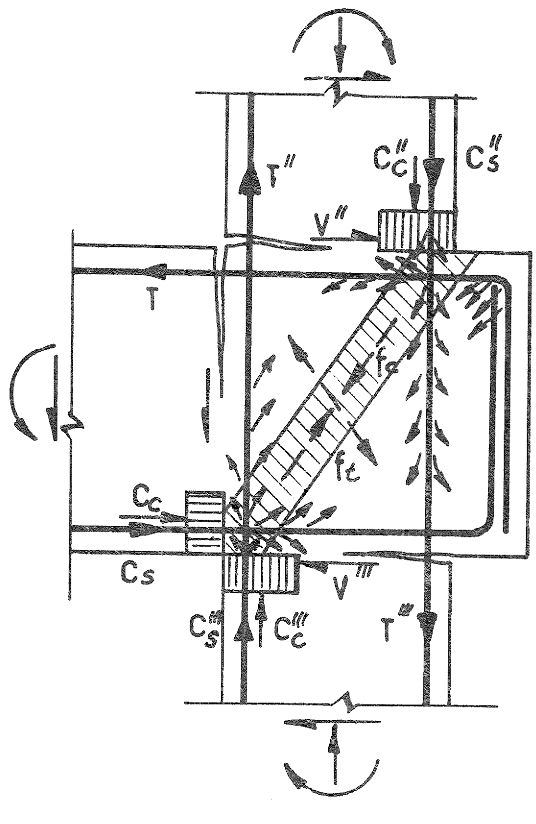

(c) Forces on External Joint

FIGURE 1: BEAM-COLUMN JOINT FORCES

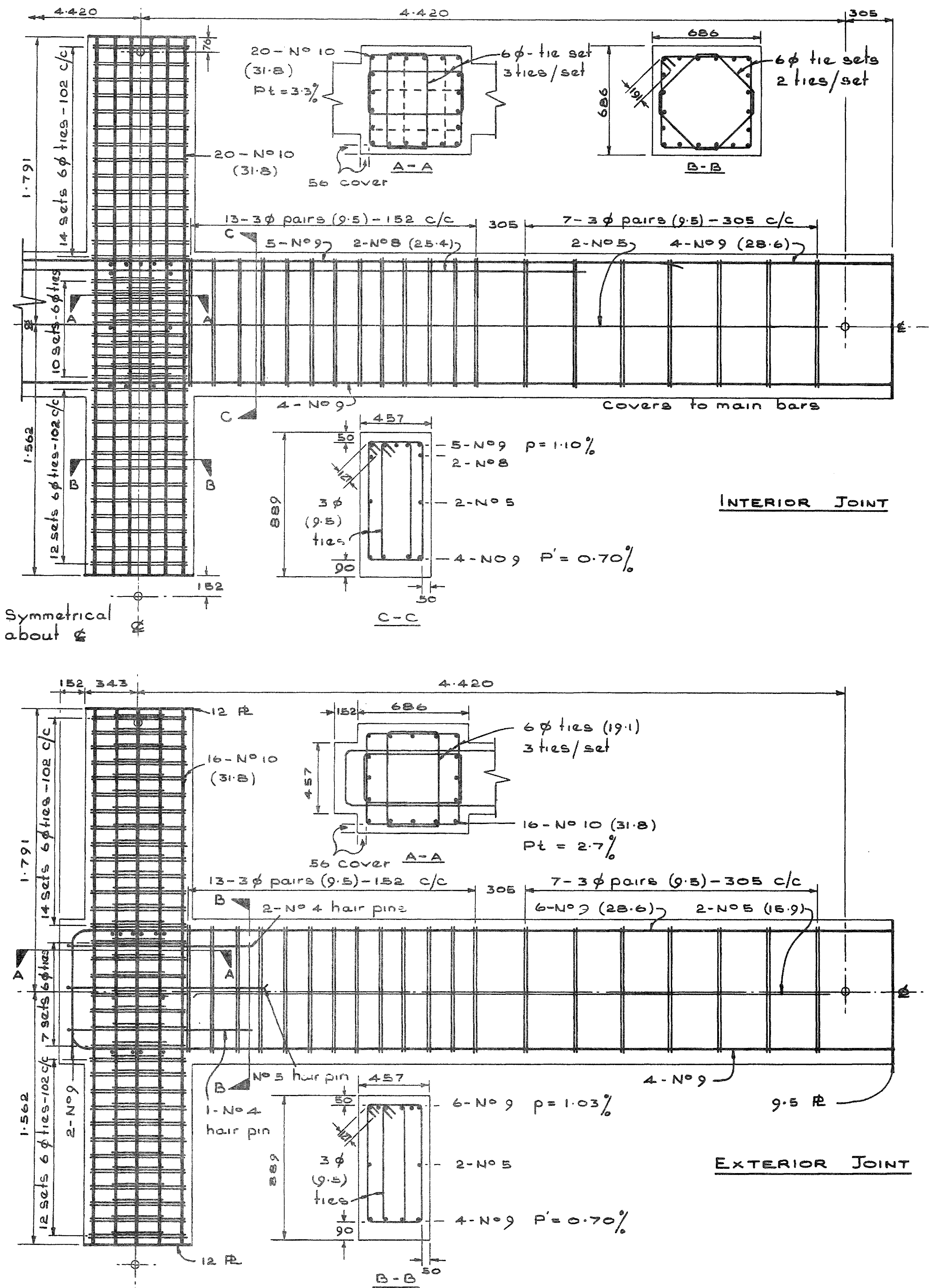

FIG 2 REINFORCING DETAILS

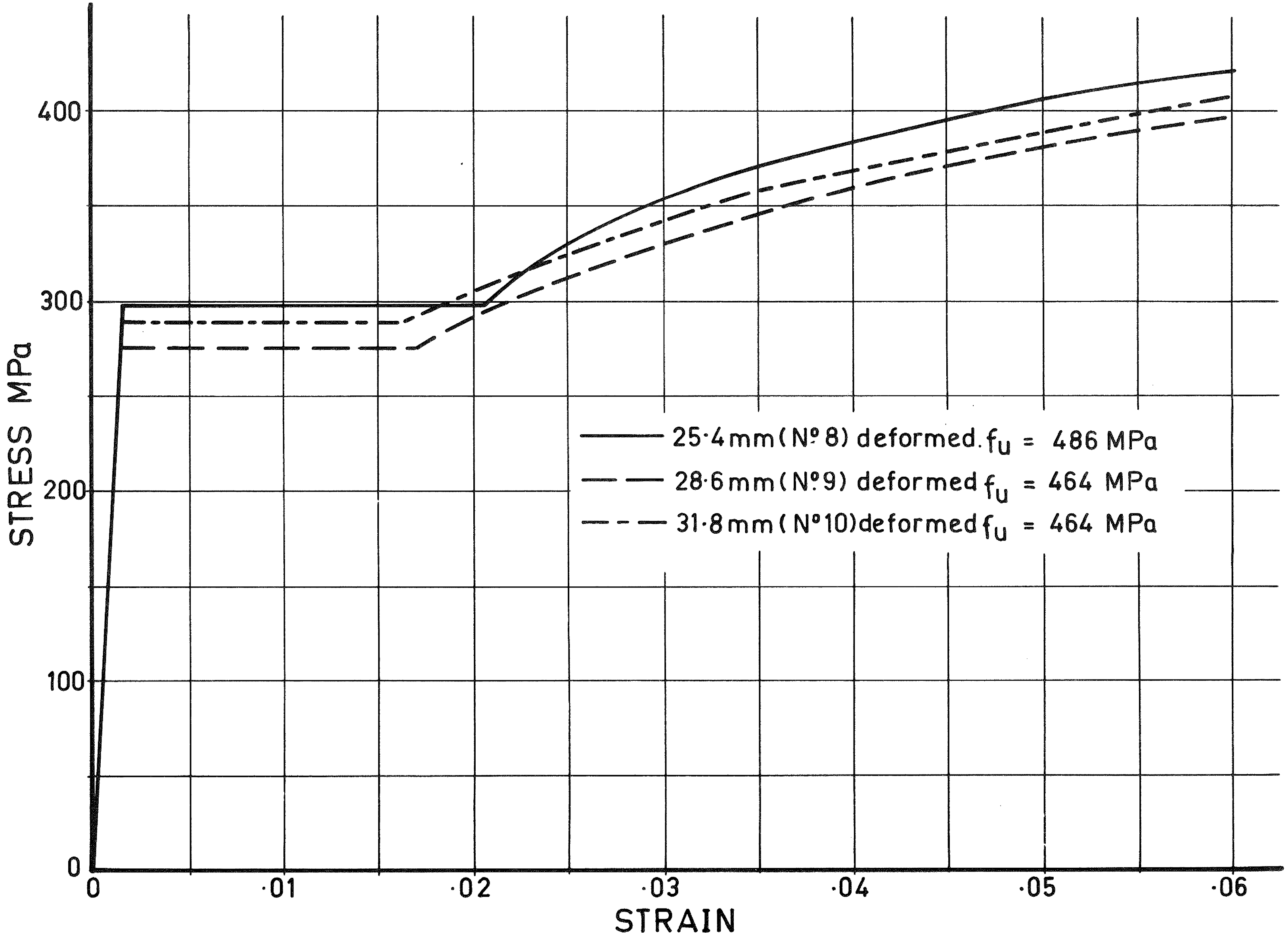

FIGURE 3: MAIN STEEL STRESS STRAIN CURVES

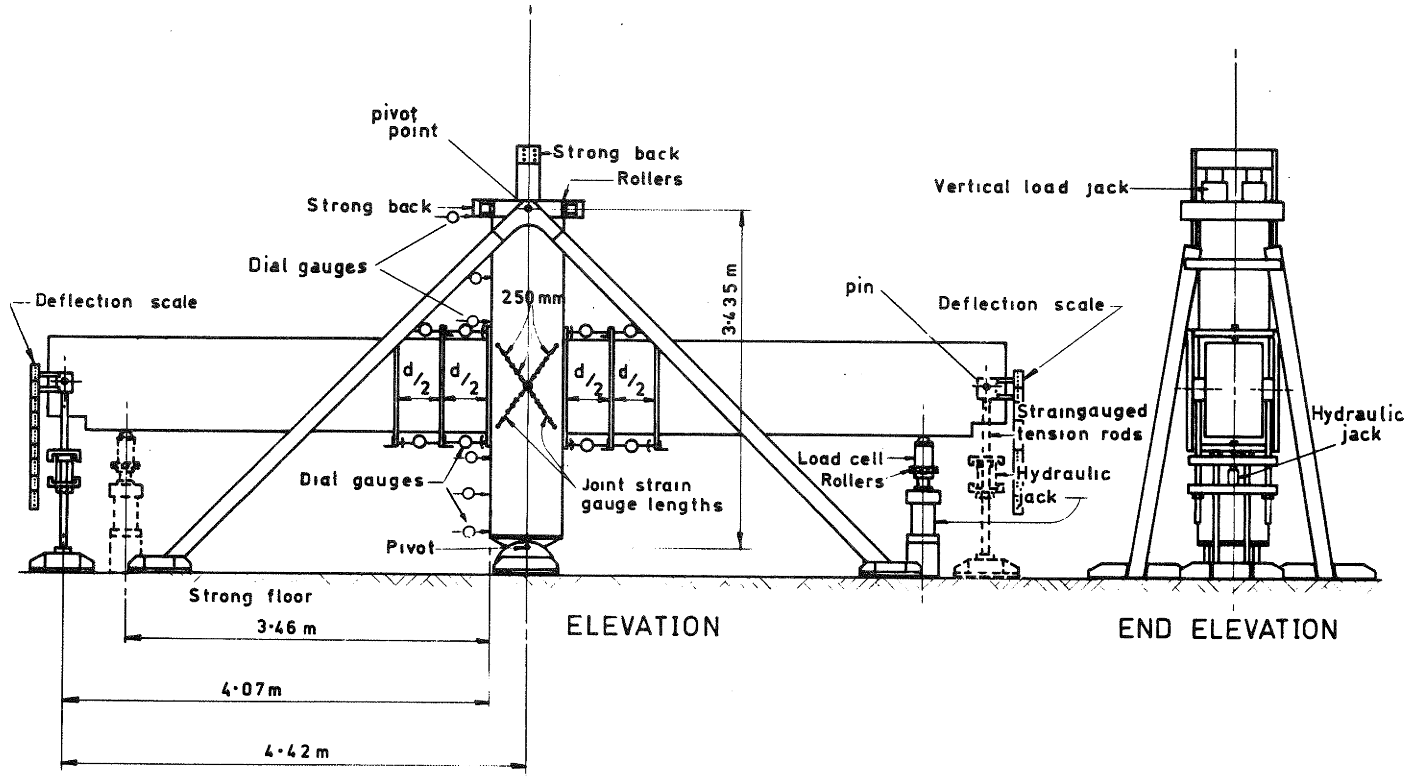

FIGURE 4: TEST SET-UP FOR INTERIOR JOINT

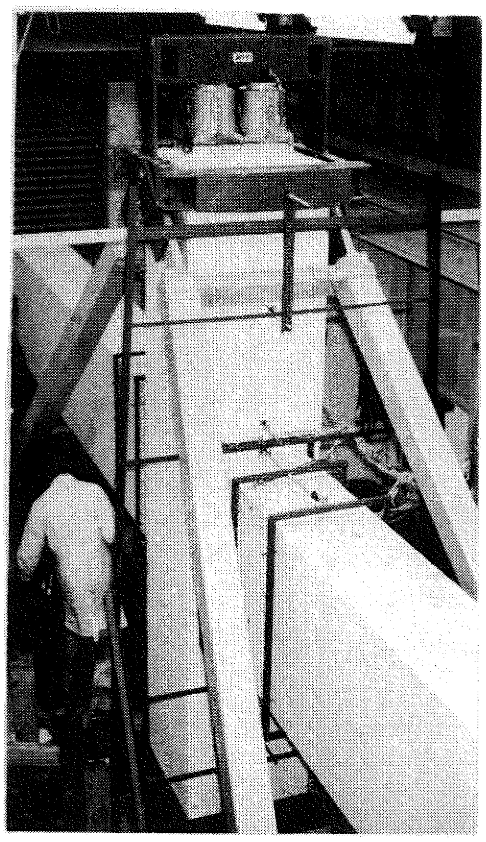

FIGURE 5: INTERIOR JOINT UNDER TEST

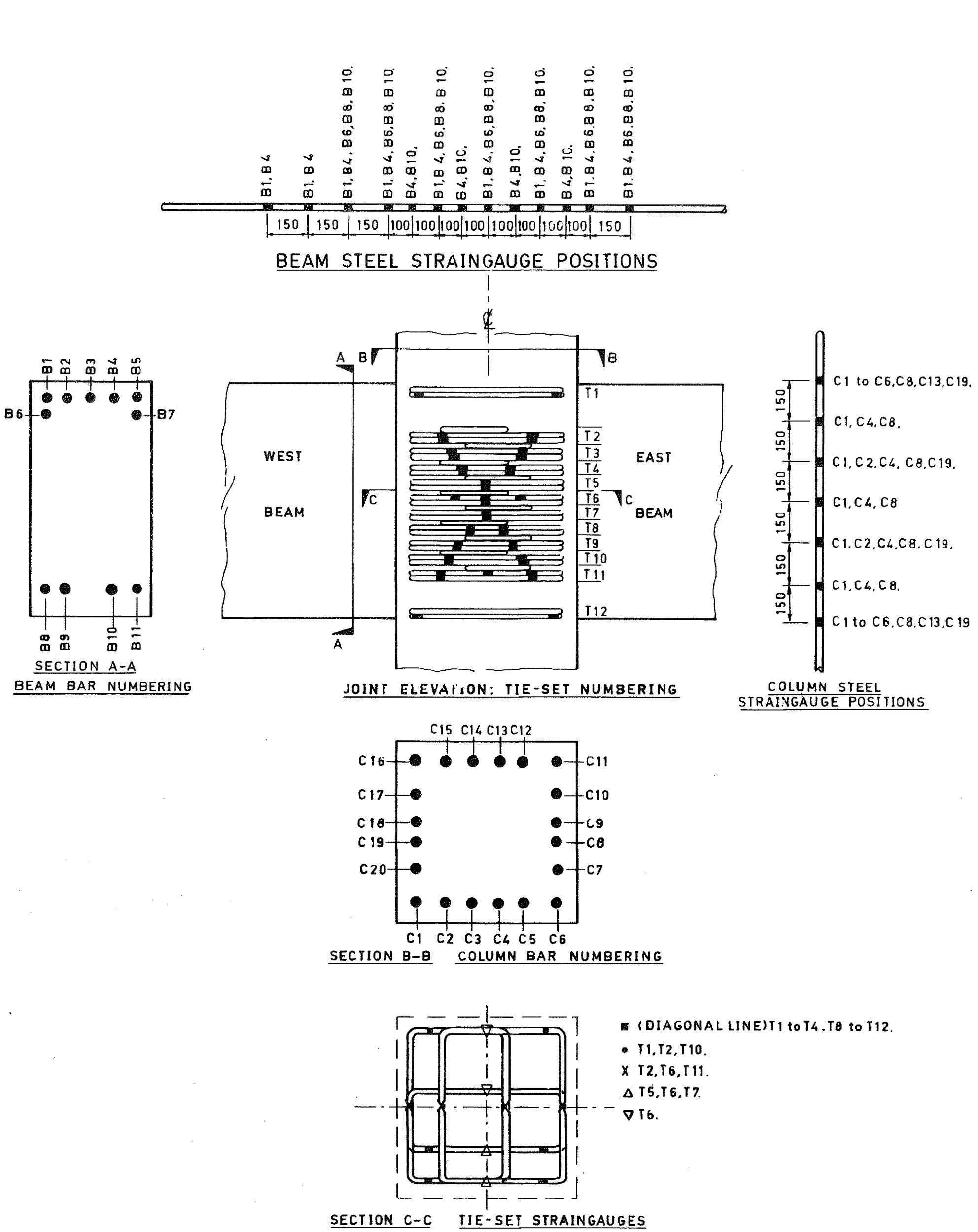

(a) INTERIOR JOINT

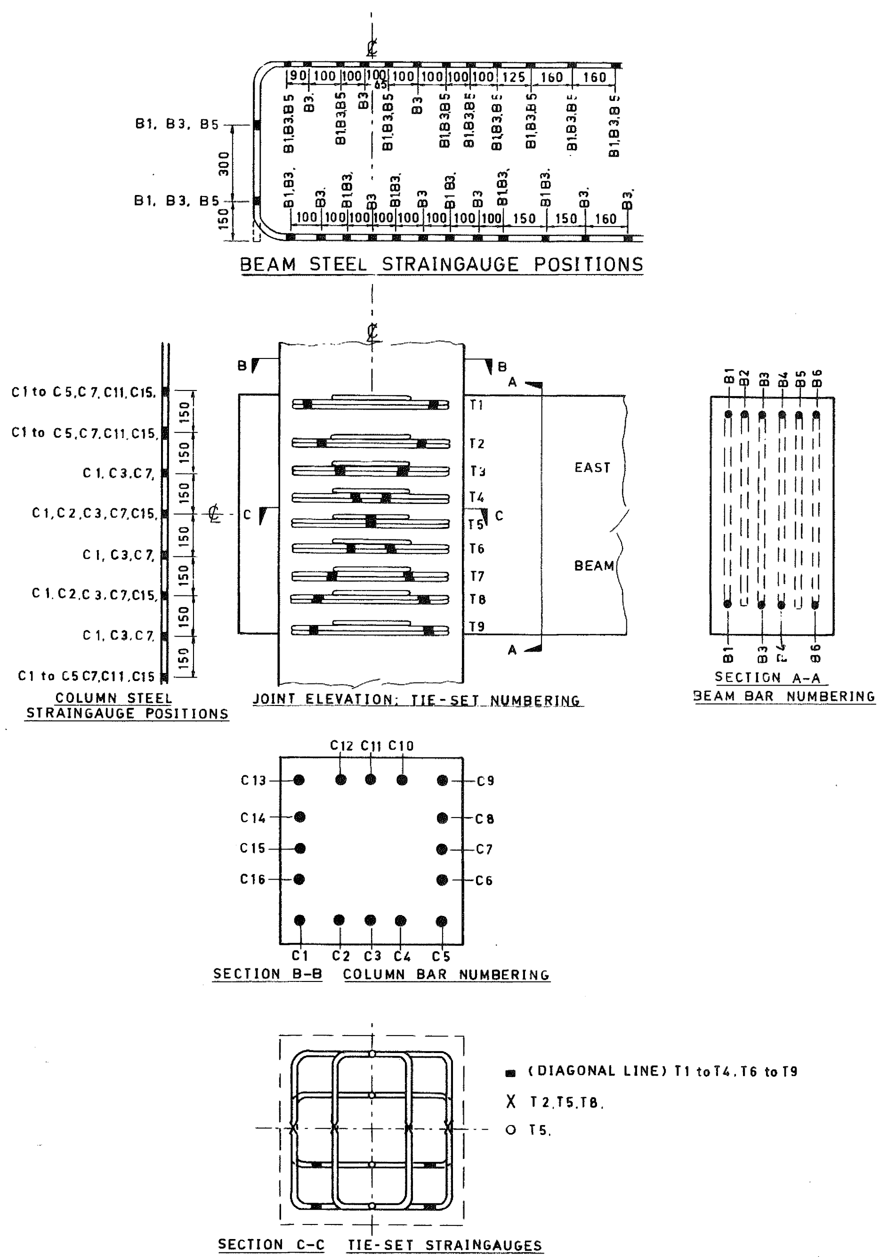

(b) EXTERIOR JOINT

DIMENSIONS IN mm

FIGURE 6: ELECTRIC RESISTANCE STRAINGAUGE POSITIONS.

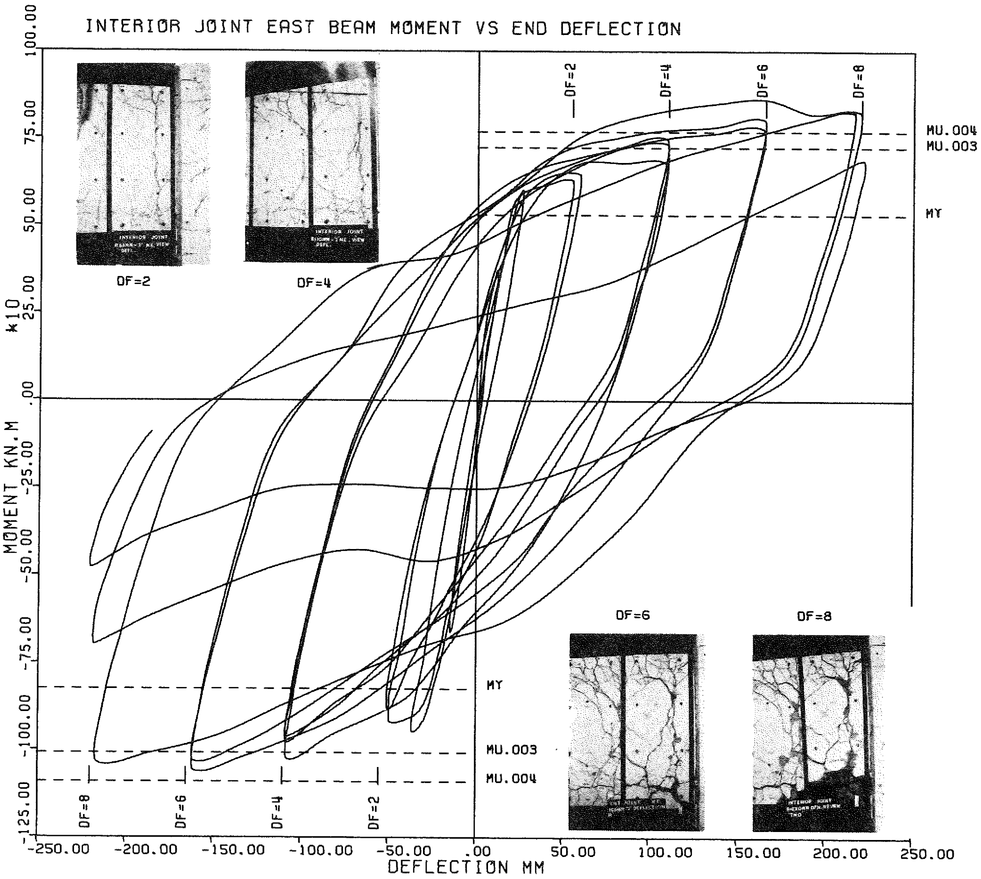

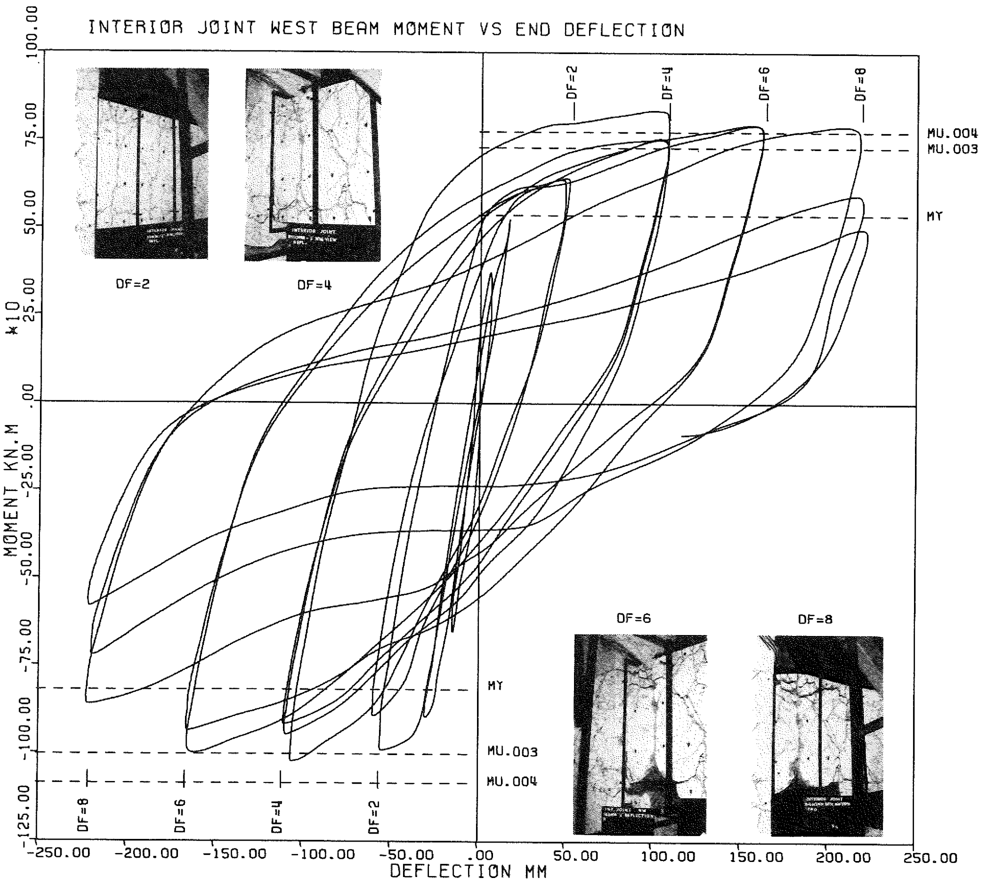

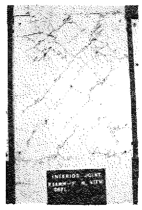
JOINT.DF=2

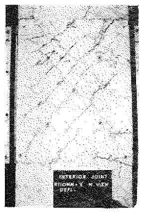
JOINT.DF=4


JOINT.DF=6


JOINT.DF=8

FIGURE 7: MOMENT-DEFLECTION BEHAVIOUR OF INTERIOR JOINT TEST UNIT.

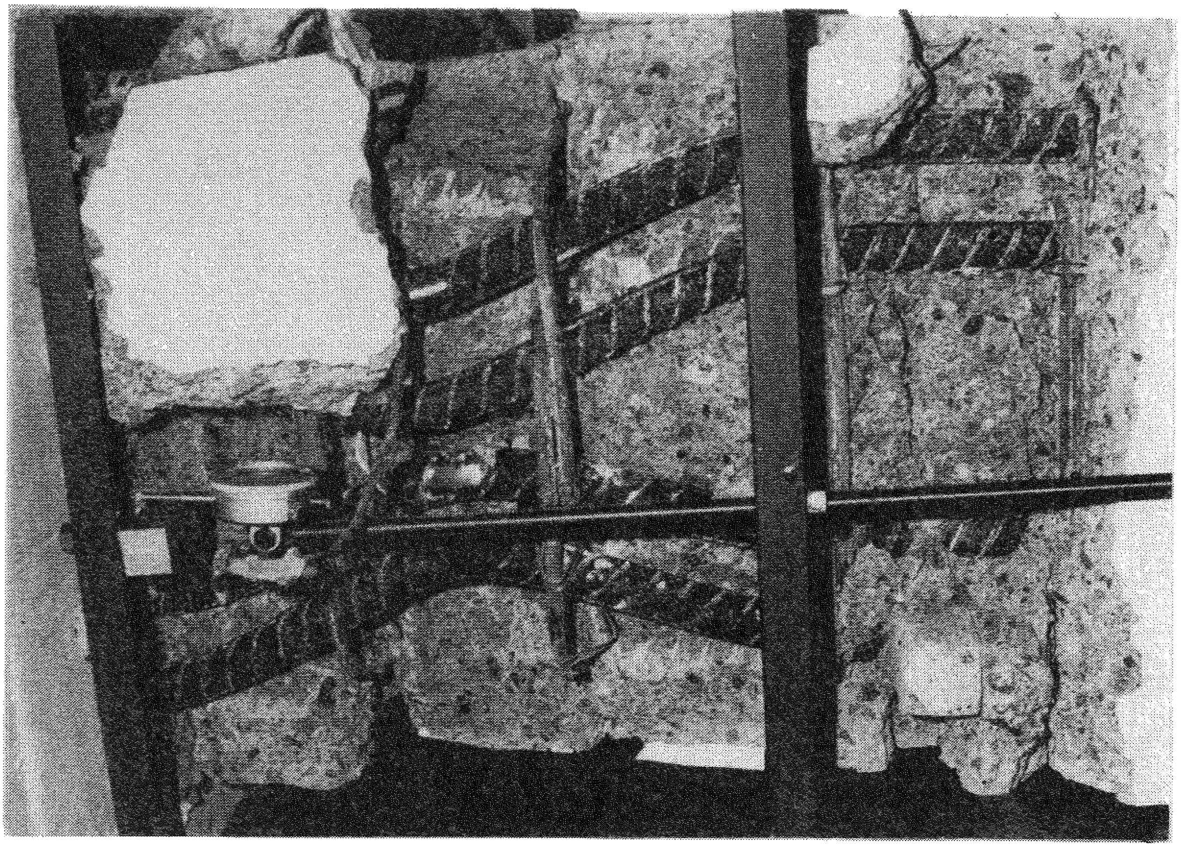

FIGURE 8: LATERAL BUCKLING OF BOTTOM BEAM STEEL. INTERIOR JOINT, DF = 8.

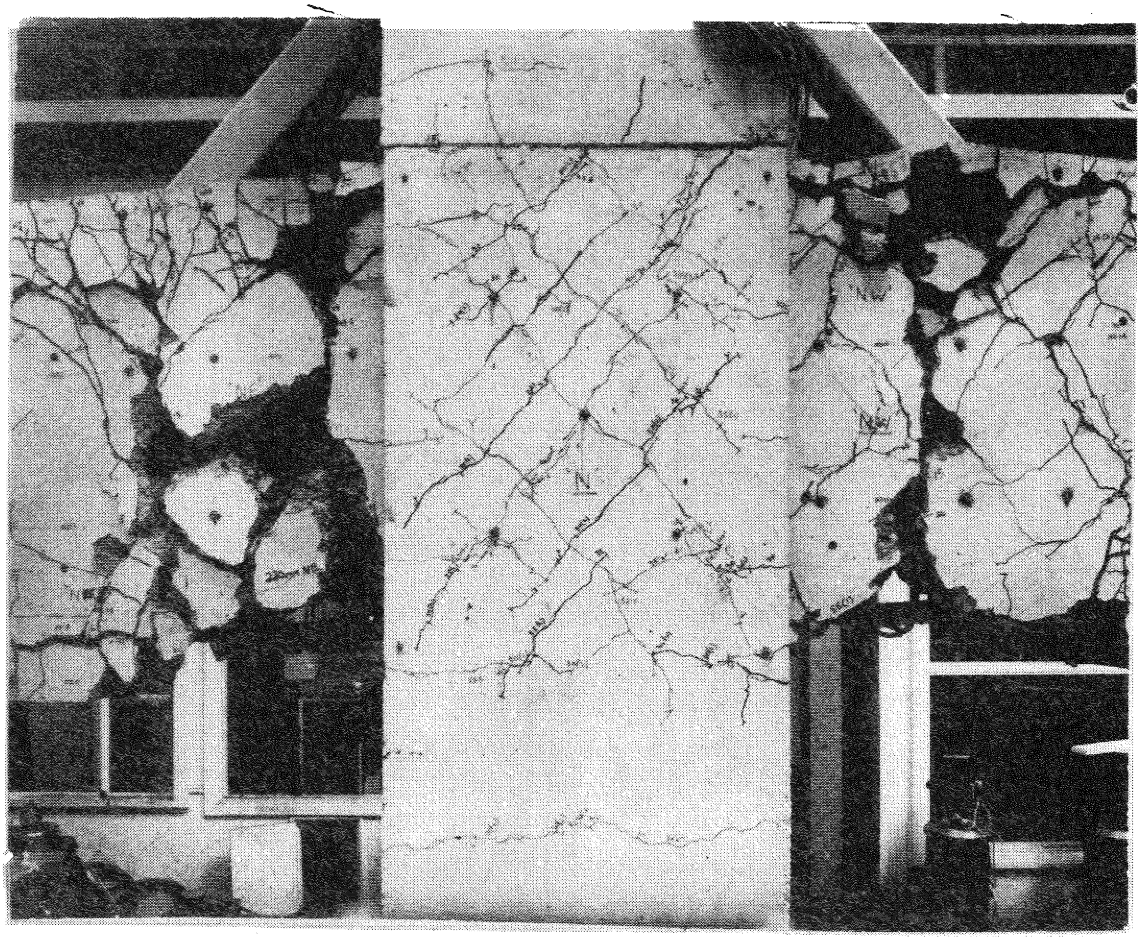

FIGURE 9: CONDITION OF INTERIOR JOINT AFTER COMPLETION OF TESTING.

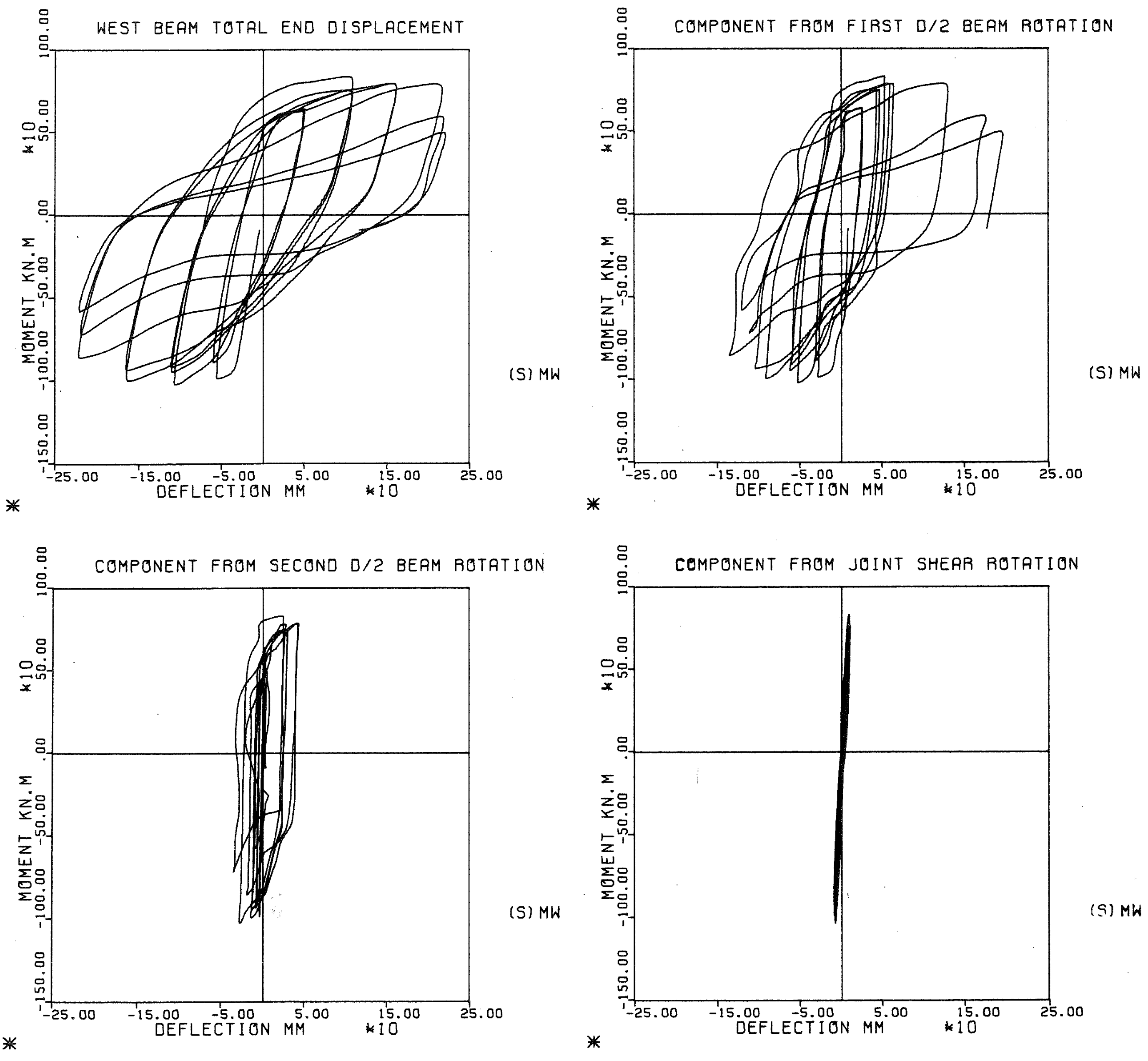

FIG.10 COMPONENTS OF WEST BEAM END DISPLACEMENT, INTERIOR JOINT TEST UNIT

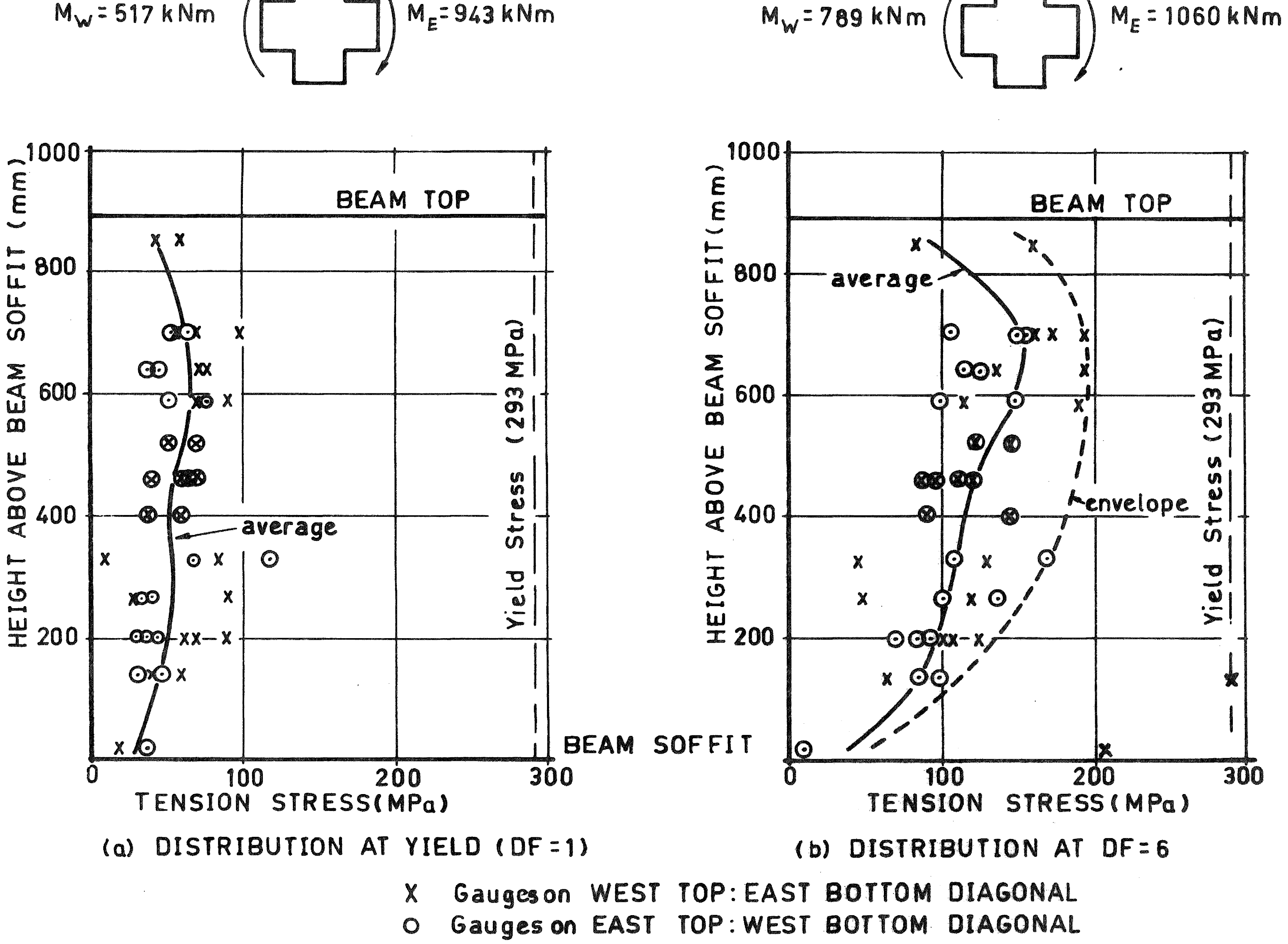

FIGURE 11: JOINT TIE LONGITUDINAL STRESS DISTRIBUTIONS. INTERIOR JOINT.

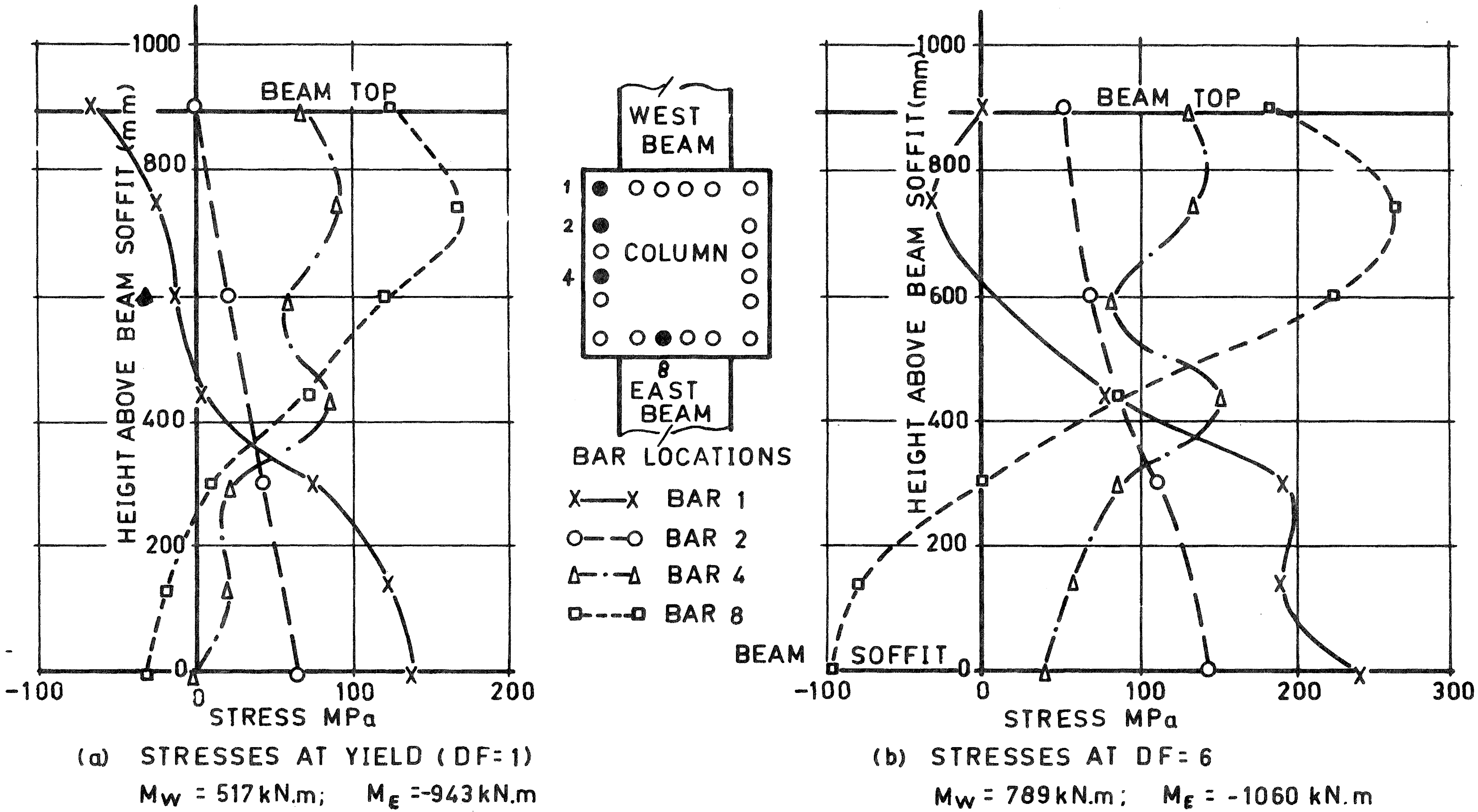

FIGURE 12: COLUMN BAR STRESSES THROUGH INTERIOR JOINT.

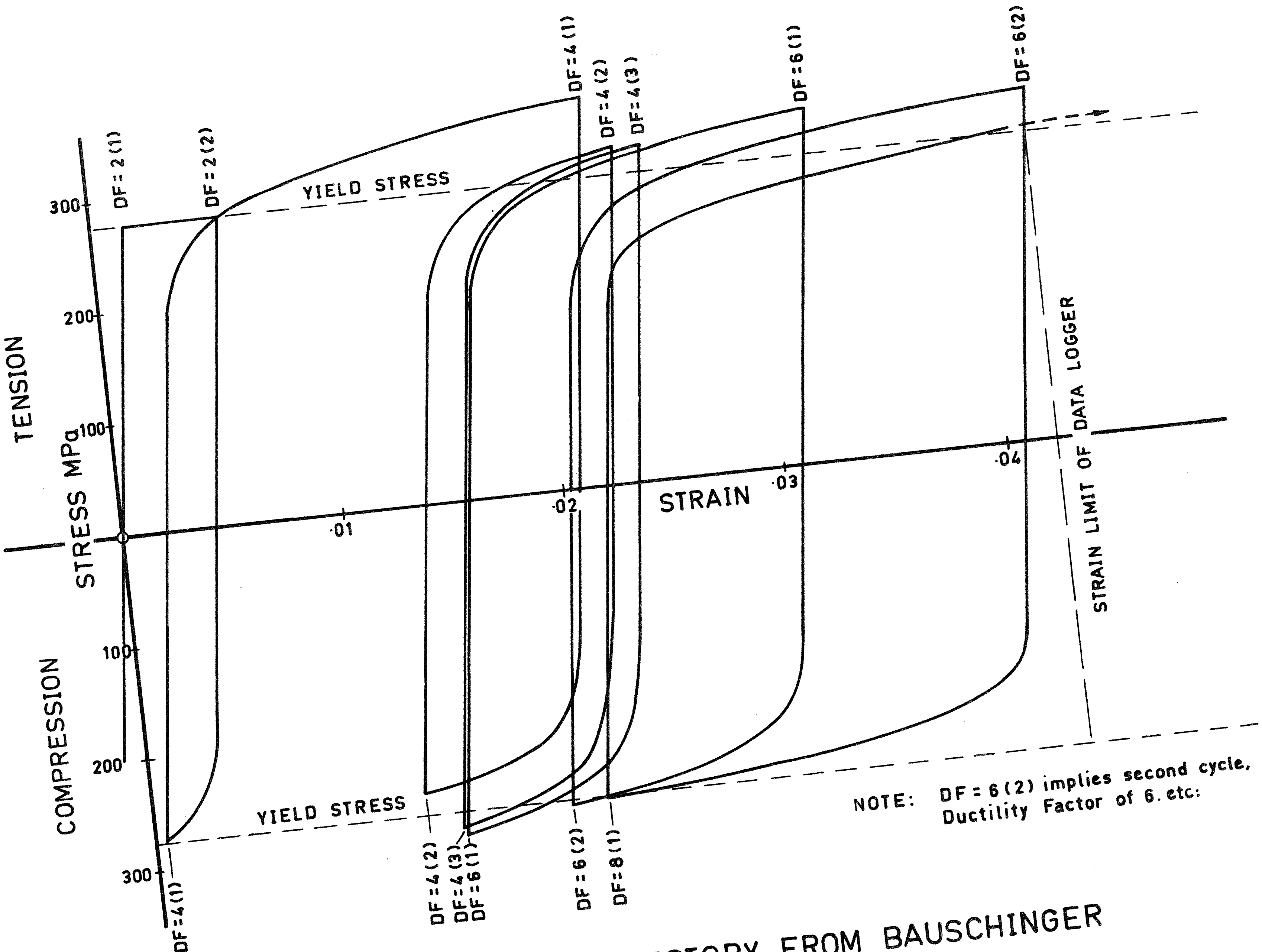

FIG: 13 TYPICAL STRESS-STRAIN HISTORY FROM BAUSCHINGER ANALYSIS. EAST BEAM TOP BAR.

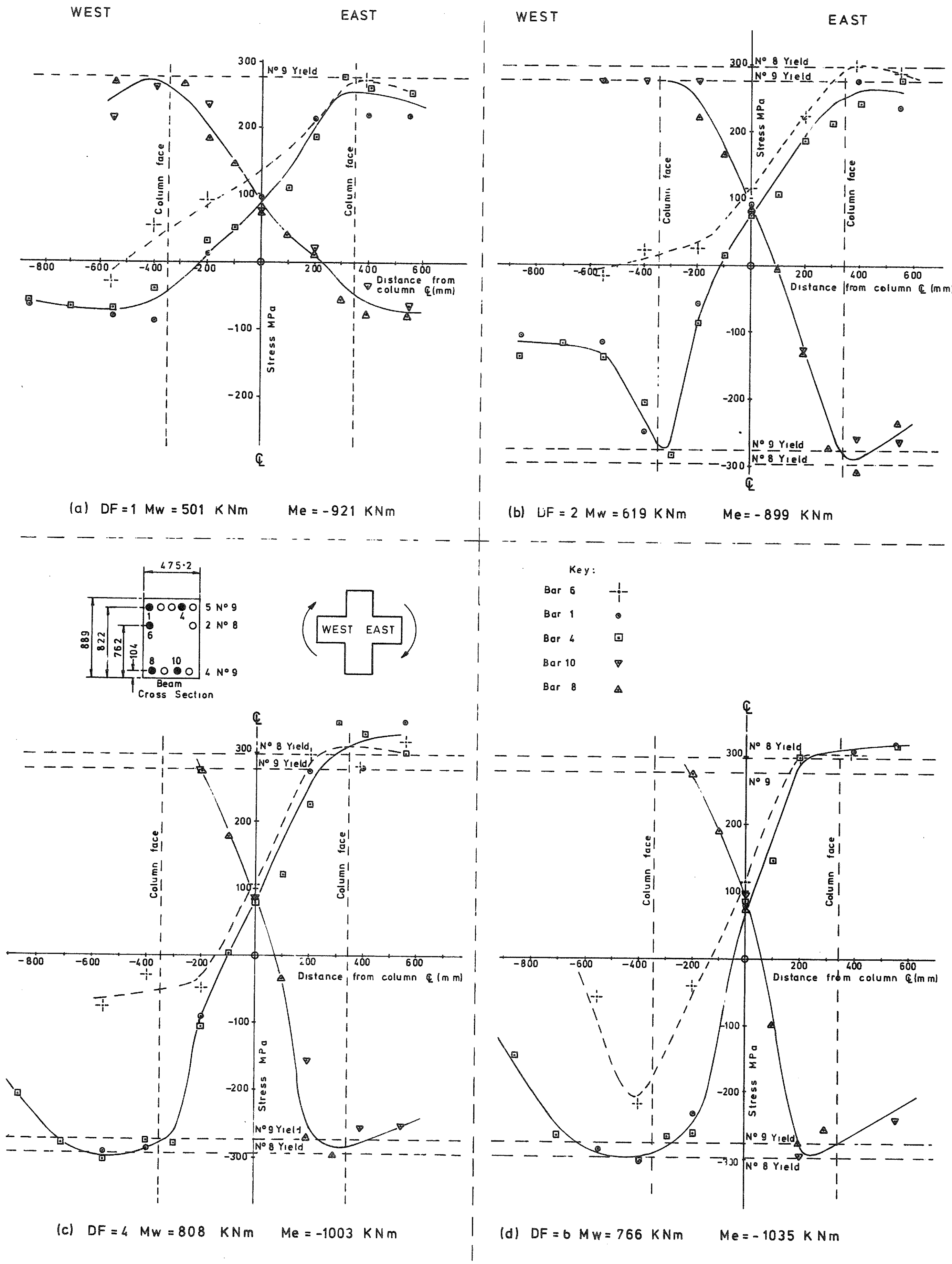

FIG: 14. BEAM STEEL STRESS DISTRIBUTIONS THROUGH JOINT

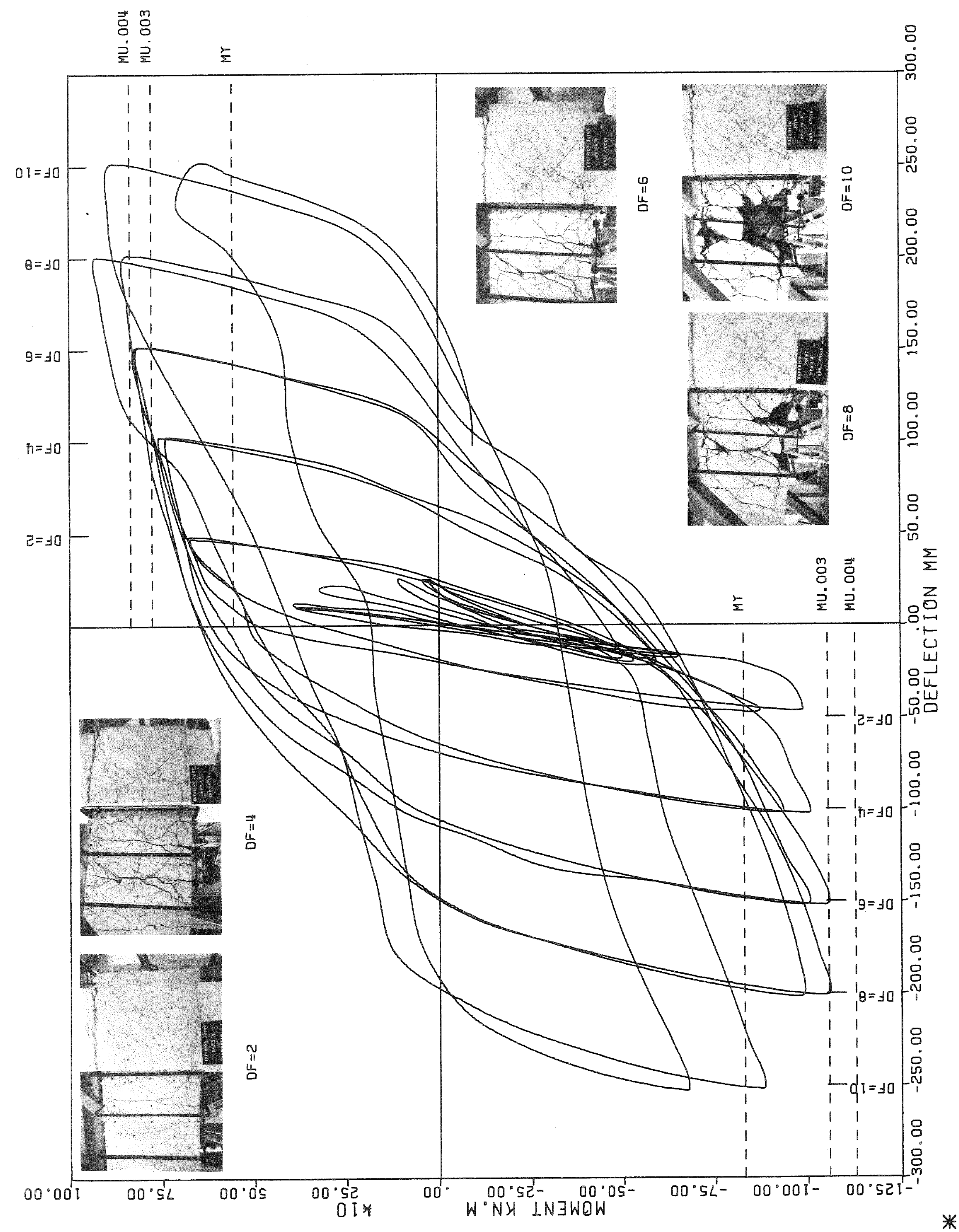

FIGURE 15: MOMENT-DEFLECTION BEHAVIOUR OF EXTERIOR JOINT TEST UNIT.

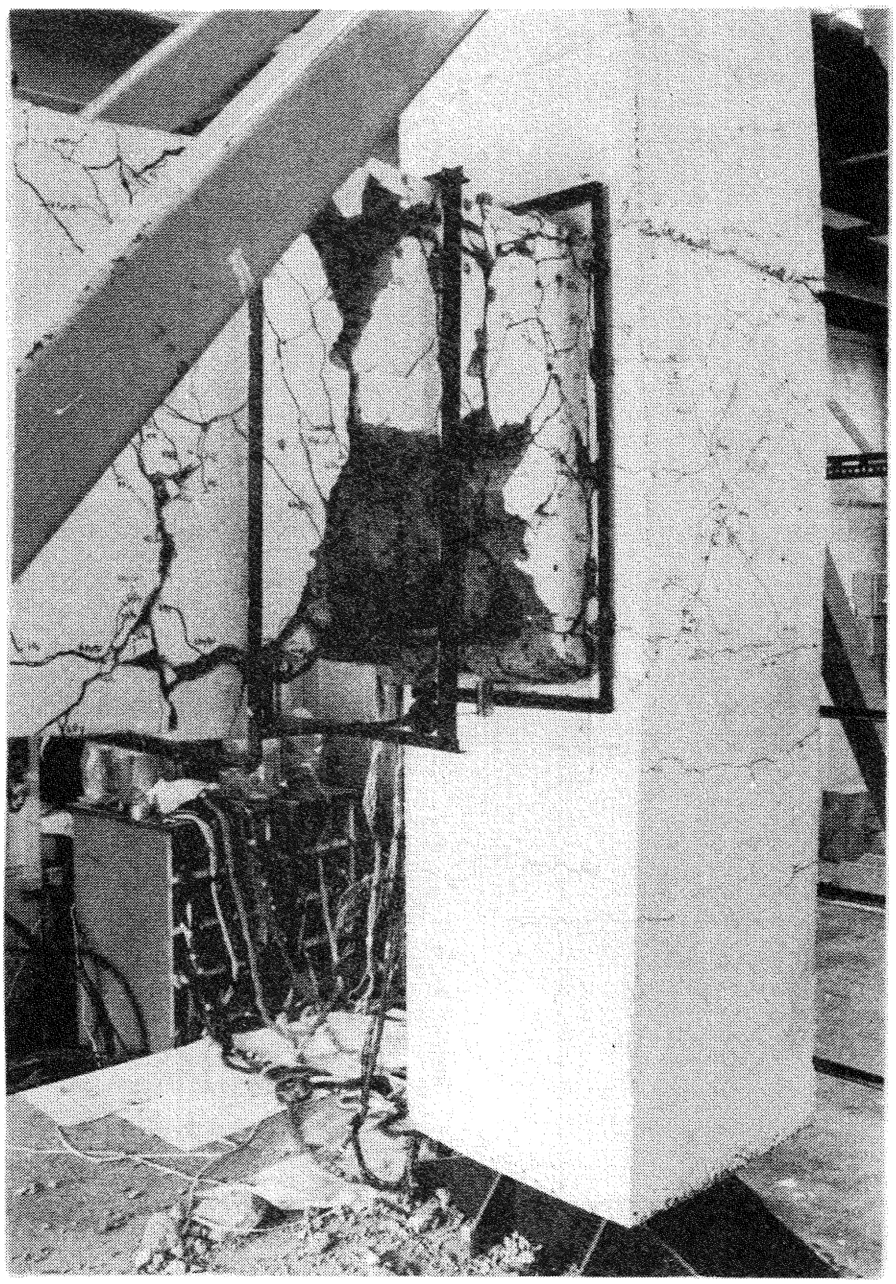

FIGURE 16: CONDITION OF EXTERIOR JOINT AFTER COMPLETION OF TESTING

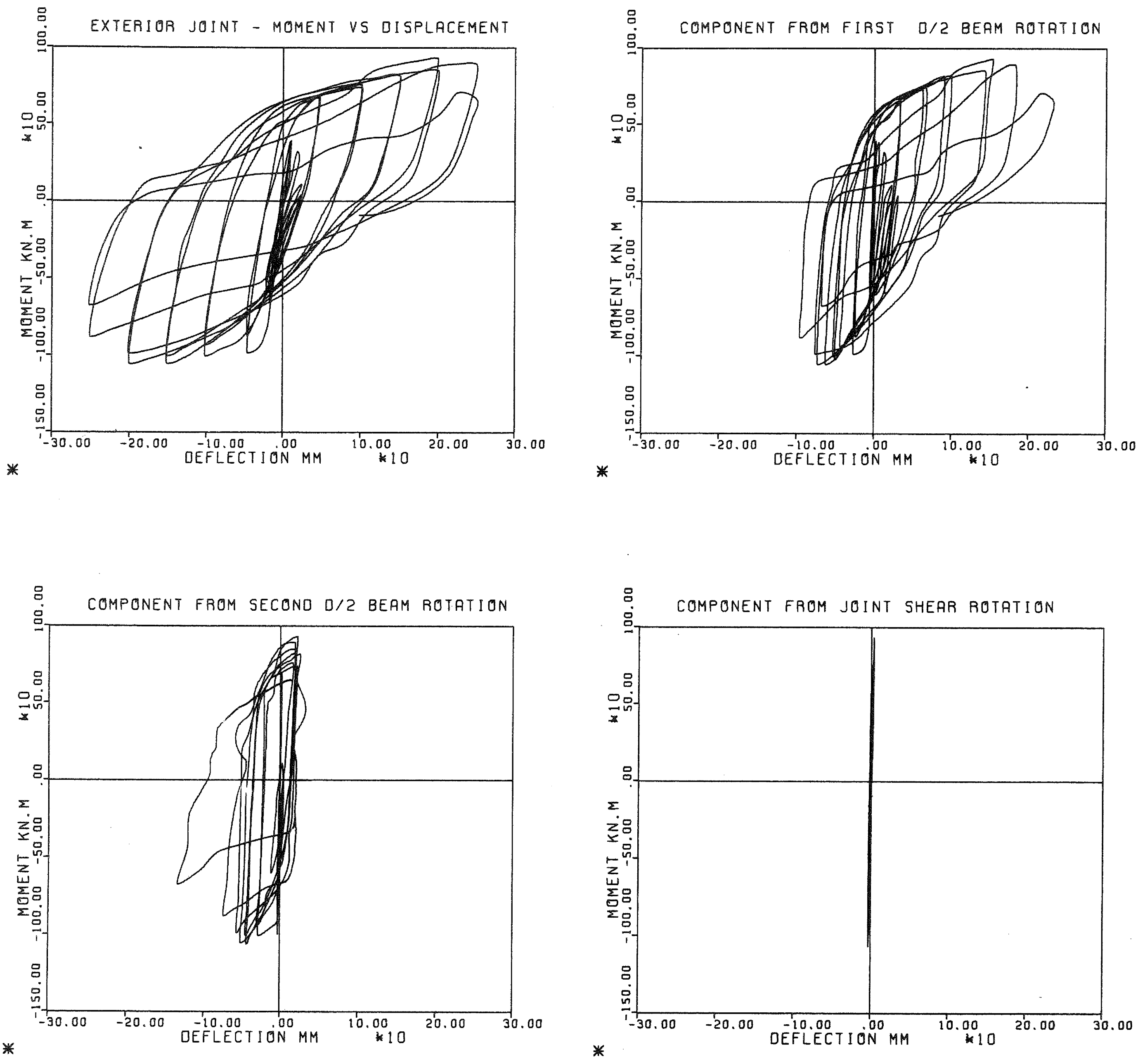

FIGURE 17: COMPONENTS OF EXTERIOR JOINT BEAM END DISPLACEMENT.

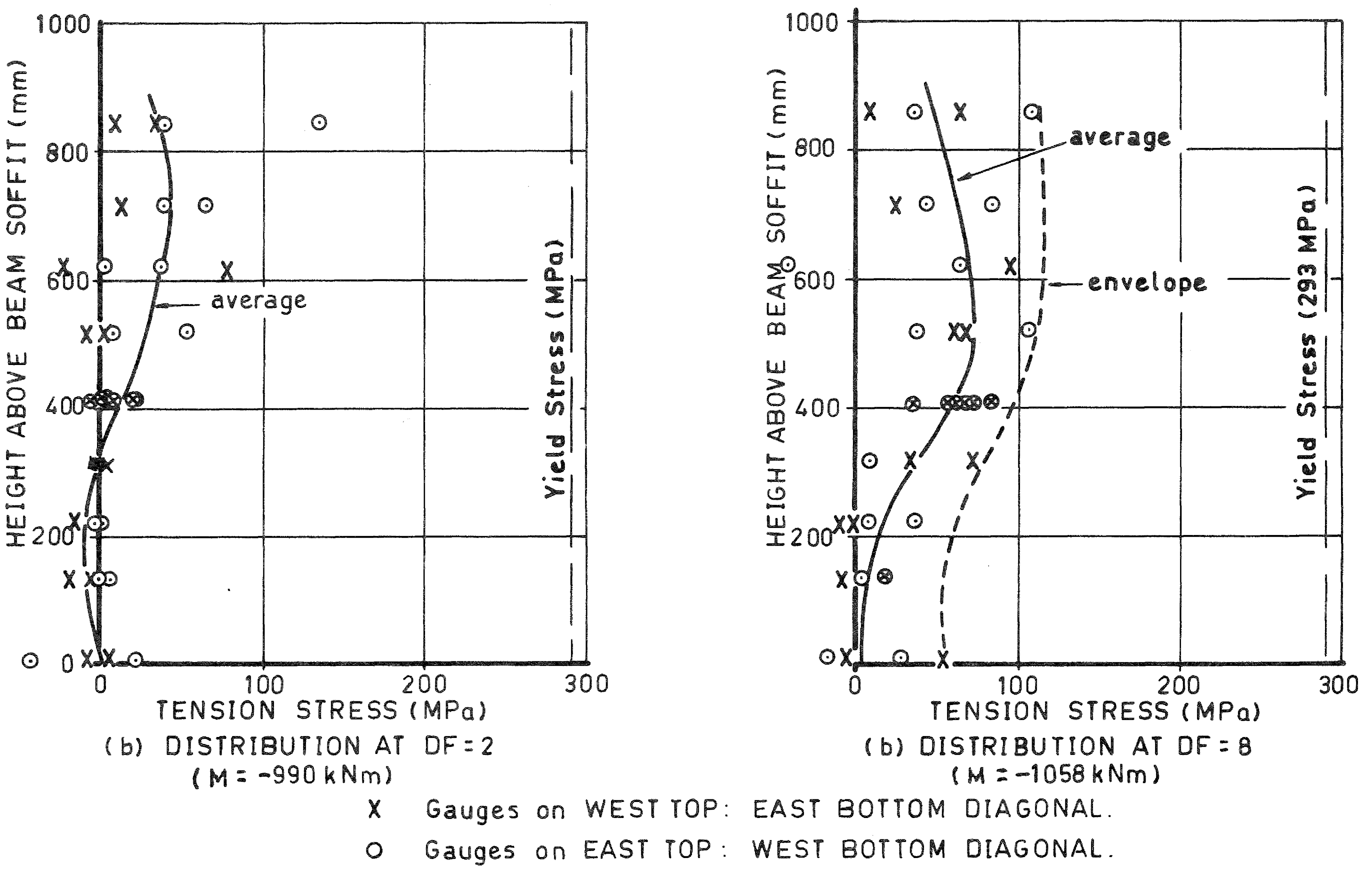

FIG: 18 JOINT TIE LONGITUDINAL STRESS DISTRIBUTIONS.
EXTERIOR JOINT

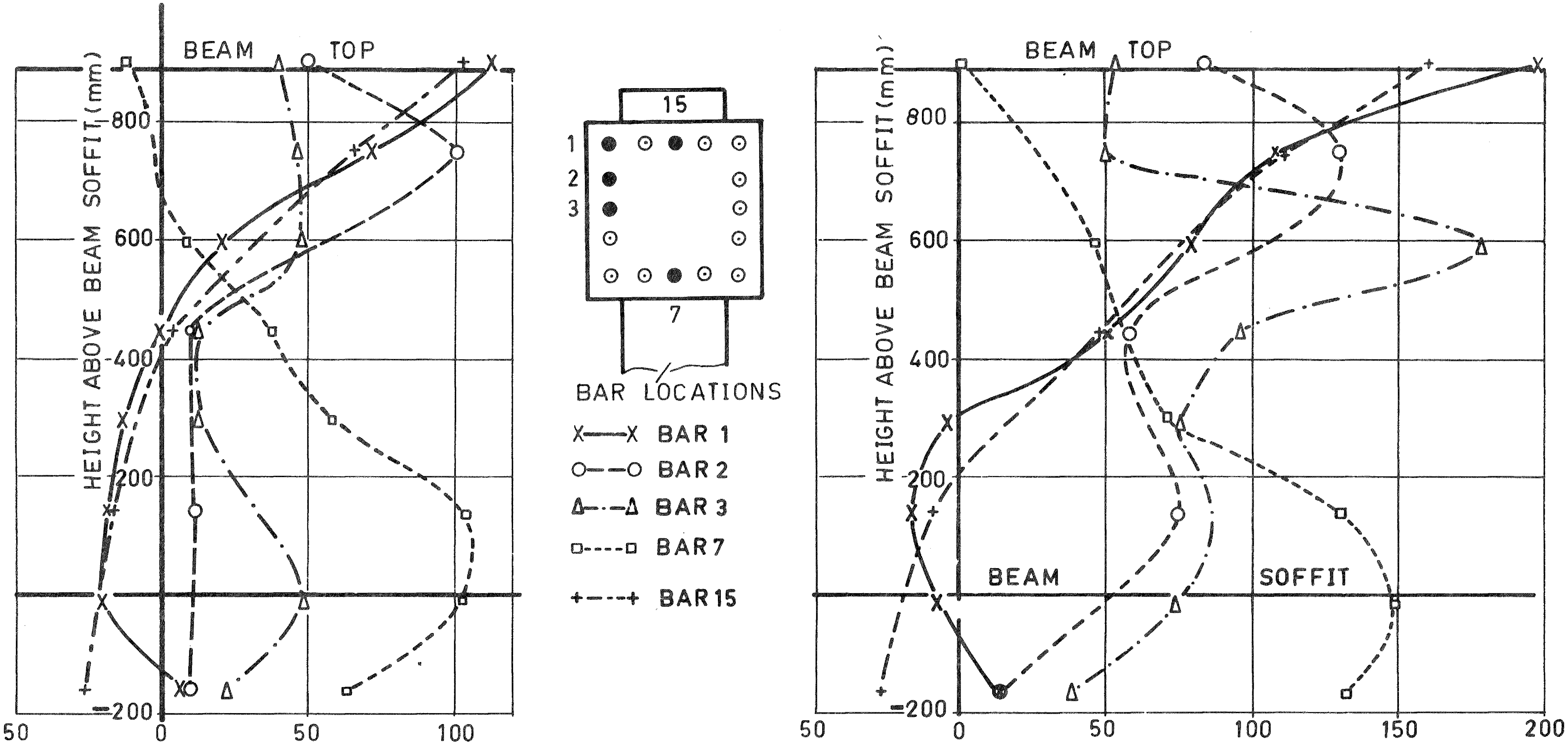

STRESS (MPa)
(a) STRESS AT DF = 2
M = 674 kN.m

STRESS (MPa)
(b) STRESS AT DF = 8
M = 853 kN.m

FIG: 19 COLUMN BAR STRESSES THROUGH EXTERIOR JOINT

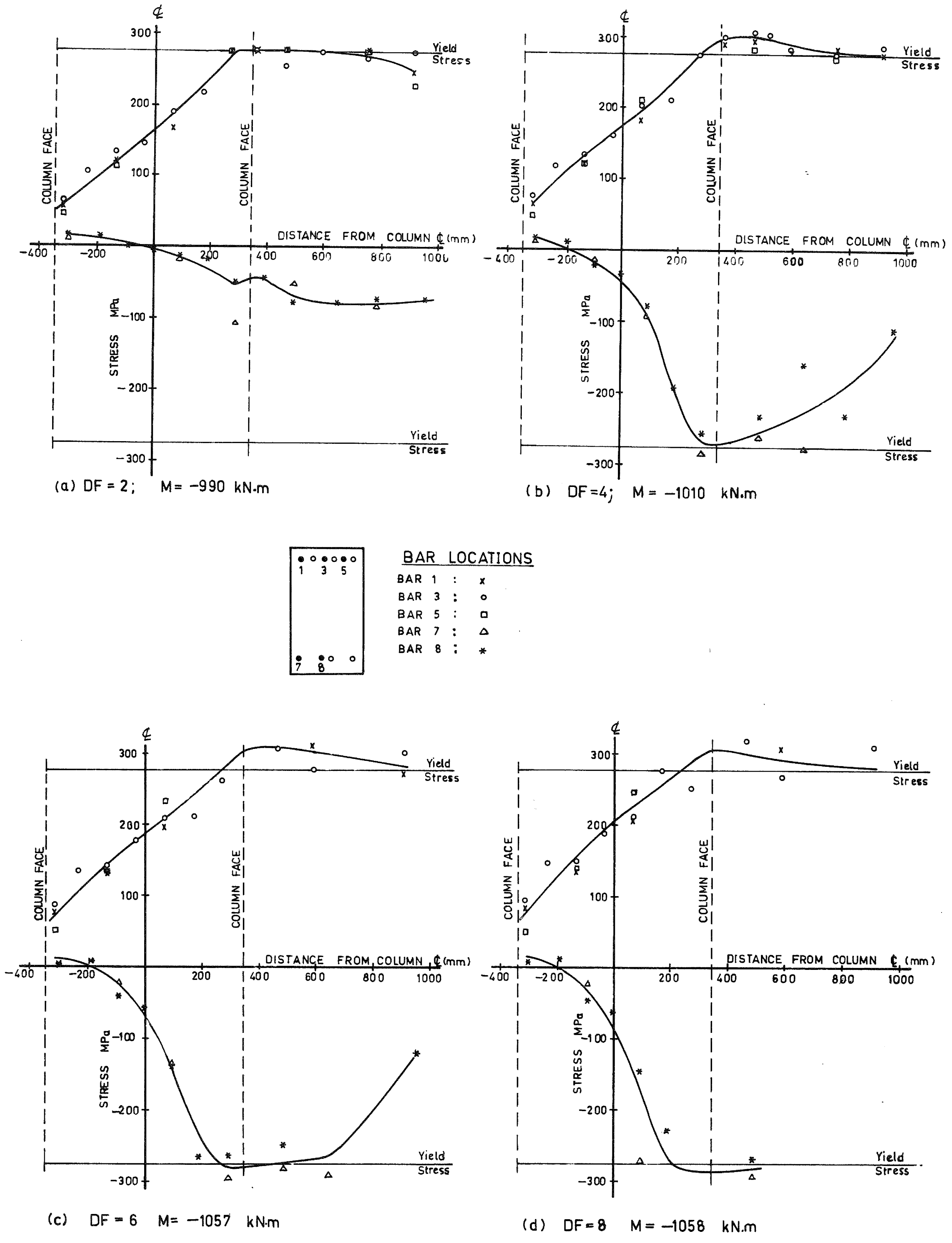

FIG. 20 BEAM STEEL STRESS DISTRIBUTIONS THROUGH EXTERIOR JOINT NEGATIVE MOMENT CONDITIONS

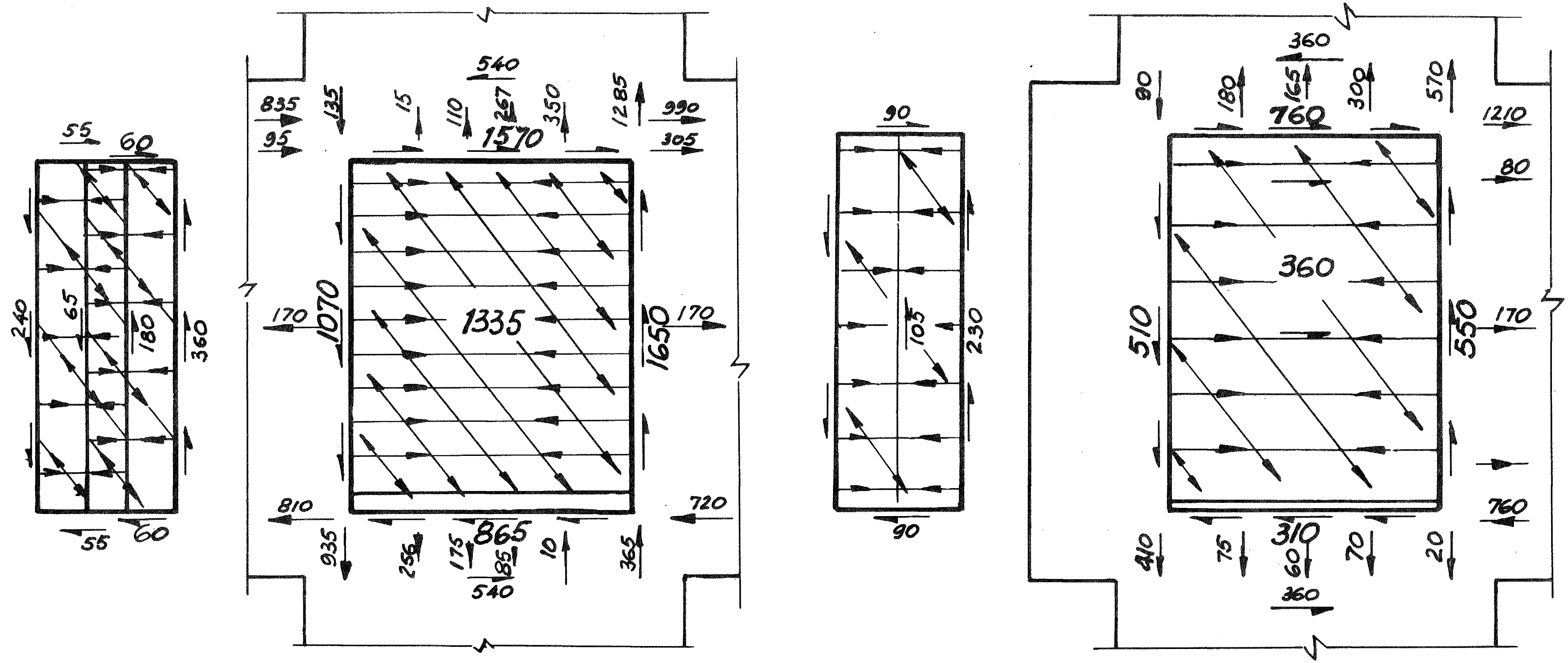

MINOR TRUSS　　　MAJOR TRUSS　　　MINOR TRUSS　　　MAJOR TRUSS

(a) Interior Joint, DF = 6　　　(b) Exterior Joint, DF = 8

Unit of Force : kN

FIG. 21 FORCES IN TRUSS MECHANISMS

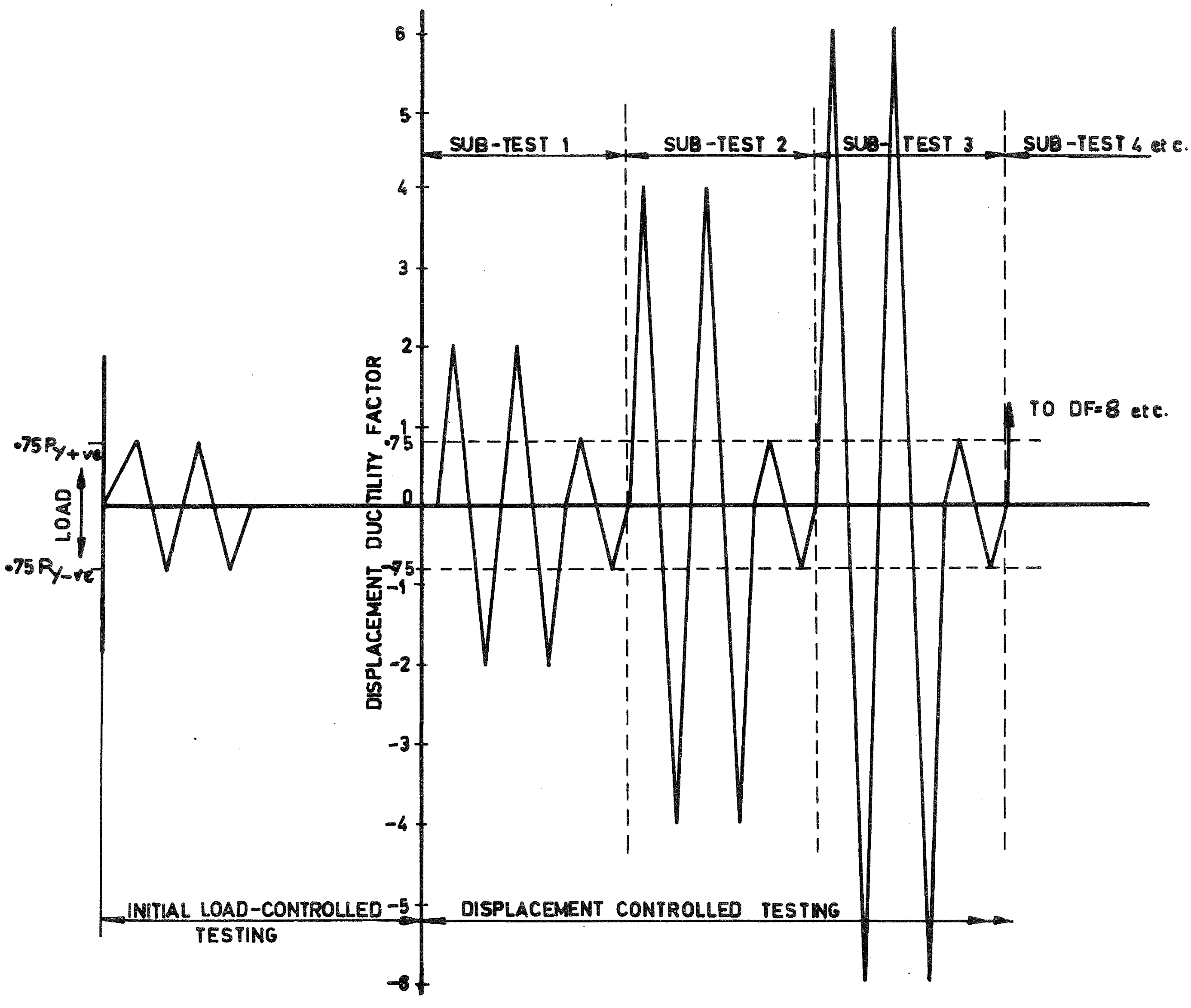

FIG. A-1
STANDARD BEAM-COLUMN TEST SEQUENCE